Doctoral Dissertation (Shinshu University)

# Studies on water based processing of electrospun silk fibroin nanofiber non-woven fabric for cell scaffold

March,2017

Yuki Kishimoto

Interdisciplinary Graduate School of Science and Technology,

Shinshu University

Department of Bioscience and Textile Technology

CONTENTS

# Chapter 1: General Introduction

## Chapter 1: General introduction

### 1. Silk fibroin and regenerated materials

Silk is a well described natural fiber obtained from silkworms and spiders and has been used in textile industries due to its luster and excellent mechanical properties [1]. Silk protein are produced as a cocoon by silkworms are classified into two general groups: domestic type (*Bombyx mori*) and wild type (*Antheraea pernyi* etc.) silkworms [1, 2]. Silk cocoons filaments from the silkworm cocoon consists of hydrophobic fibroin (SF) and hydrophilic sericin.

The domesticated silkworm (*B. mori*) SF fibers are about 10-25 μm in diameter and consist of two proteins: a light chain (~25 kDa) and heavy chain (~400 kDa) which are present in a 1:1 ratio and linked by a single disulfide bond [1]. These proteins are coated with sericin (20–310 kDa) [1]. The disulfide linkage between the Cys-c20 (twentieth residue from the carboxyl terminus) of the heavy chain and Cys-172 of the light chain holds the fibroin together and a 25 kDa glycoprotein, named P25, is noncovalently linked to these proteins [1].

SF fiber can be extracted from cocoon by boiling silk cocoons in an alkaline solution. Twenty five to thirty percent of the silk cocoon mass is sericin which is removed during degumming process [3]. Degumming is the first step in silk fibroin processing. To prepare silk solution for regenerated different silk fibroin materials, concentrated aqueous solutions of LiBr [4], $CaCl_2$ [5], LiSCN [6] and ionic liquid [7] are commonly used for dissolving of SF fiber. The SF aqueous solution can be produced through dialysis process of above SF solutions [4]. Regenerated SF materials such as film [8], hydrogel [9], 3-D sponge [10] and electrospun SF nanofiber non-woven fabric [11] are formed by SF

aqueous solution or SF organic solutions (Table1.).

Regenerated SF materials has been extensively studied as one of the promising materials for tissue engineering applications such as cell scaffold, cartilage regeneration and artificial blood vessel and so on, because it has several biological properties including good biocompatibility, biodegradability, minimal inflammatory reaction, and mechanical properties [26-29].

**Table.1** Different form of regenerated SF materials and applications.

| Form | Application | References |
|---|---|---|
| Film | Would dressing | [12] |
| Film | Bone regeneration | [13-15] |
| Film | Hepatic regeneration | [16] |
| Film | Antithrombogenesis | [17] |
| Hydrogel | Bone regeneration | [18] |
| Sponge | Would dressing | [19] |
| Sponge | Cartilage regeneration | [20-23] |
| Nanofiber fabric | Artificial blood vessel | [24,25] |

## 2. Electrospinning technology

Electrospinning is a one of the fabrication method of fibers with diameters ranging from 10 nm to several micrometers using polymer solutions of both natural and synthetic polymers [30]. In the electrospinning process, a high voltage is applied to create and electrically charged jet of polymer solution. The polymer jet are collected on a ground as a non-woven fabric.

The typical electrospinning setup and SEM image of nanofiber fabric are shown in Fig.1. Basically, an electrospinning setup consists of three major components: a high voltage supplier, a syringe with needle and a grounded fiber collector (flat plate or rotating drum). The polymer solution is applied into a syringe which is equipped with a piston and a stainless steel needle serving as electrode and pushed by a pump with a defined flow rate. The needle is connected with the high voltage (10 to 50 kv) to the polymer solution. The polymer solution held by its surface tension at the end of a needle is subjected to an electric field and an electric charge is induced on the polymer solution surface. When the electric charge applied on the polymer solution reaches a critical value, the repulsive electrical force overcome the surface tension of polymer solution. Finally, the charged polymer jet is ejected from the tip of the Taylor cone and unstable and a rapid whipping of the jet occurs in the space between the tip and collector which leads to evaporation of the polymer solvent.

The production of nanofiber by the electrospinning process is influenced by the spinning solution parameters (concentration and viscosity of polymer solution, molecular weight, surface tension, and conductivity), processing conditions (applied voltage, flow rate, and needle to collector distance), and ambient environment (temperature and humidity) [30]. The collector can be made in any shape according to the requirements,

such as rotating drum, flat plate, and parallel plate [31].

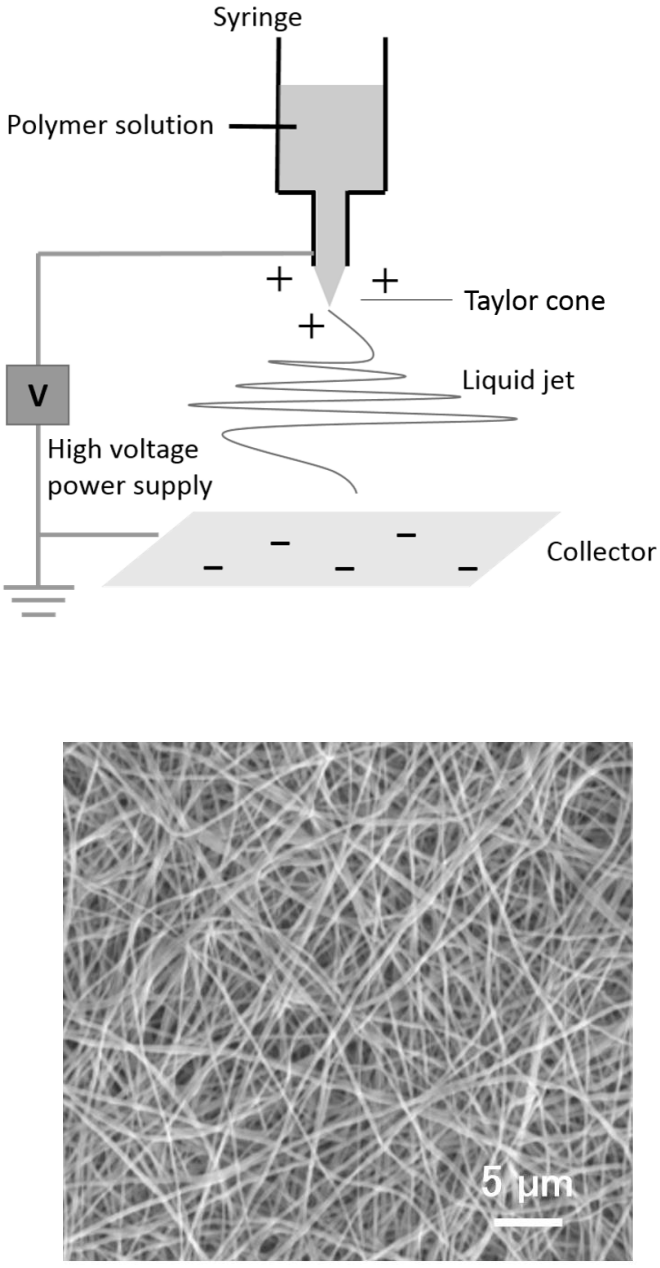


**Fig.1.** Electrospinning set up and SEM image of electrospun nanofiber non-woven fabric

### 3. Electrospun SF nanofiber non-woven fabrics

Electrospun SF nanofiber non-woven fabric has been extensively studied as one of the promising materials for tissue engineering due to its good biocompatibility, biodegradability, minimal inflammatory reaction and large surface area to volume [1, 11, 30]. These properties of SF nanofiber non-woven fabric and their potential have generated an interest in SF form various type of silkworm cocoons [11], spider dragline silk [32] and recombinant hybrid silk like polymers [33].

The relationship between type of silkworm cocoons, SF concentration, solvent, fiber diameter and mechanical properties of SF nanofiber non-woven fabrics had been discussed in many studies [11, 34-55]. The related parameters for electrospinning of silk fibroin are summarized in Table.2.

**Table.2**. Preparation conditions of SF spinning solution for electrospinning.

| Concentration of SF (wt%) | Solvent | Fiber diameter (nm) | Tensile strength (MPa) | Reference |
|---|---|---|---|---|
| 20 | Formic acid | 250 | 12 | [48] |
| 10-14 | Formic acid | 45-380 | 11-18 | [49] |
| 17 | HFIP | 850-1343 | 6-9 | [50] |
| 8 | HFIP | 440 | 1 | [51] |
| 7 | HFIP | 250-550 | 1-4 | [52] |
| 8 | PEO/Water | 700 | 13 | [53] |
| 34 | Water | 1000 | 2 | [42] |
| 33 | Water | 1400 | 6 | [55] |
| 17 | Water | 490 | 6 | [40] |
| 3-7 | HFA | 100-1000 | | [34] |

In 1998, Zarkoob et al. [56] were the first to report that SF nanofiber non-woven fabrics from *Bombyx mori* silk cocoon and spider dragline silk from *N. clavipes* can be electrospun into nanofiber fabrics with hecafluoro propanol (HFIP) as a solvent. Ohgo. [34] et al. demonstrated that the relationship between fiber characteristics and spinning solution in hexafluoroacetone (HFA) from *Bombyx mori* SF and *Samia Cynthia ricini*. Afterwards, Sukigara et al. [57-59] reported that the effect of electrospinning parameters (applied voltage, needle-to-collector distance and SF concentration) on the morphology and fiber diameter of SF nanofiber non-woven fabrics from *Bombyx mori* using formic acid as a solvent and found that the SF concentration is the most important factor in producing uniform fibers less than 100 nm in diameter.

## 4. Functionalized SF materials

In recent years, organic-inorganic composite materials have gained considerable attention because they exhibit properties that are significantly different to the corresponding bulk materials, such as high strength, improved thermal properties and enhanced surface reactivity [60-62].

SF-silica particles were reportedly produced by combining SF with silica particles and have been used as an osteoinductive composite for bone regeneration [63]. Another SF-silica composite was prepared by sol–gel crosslinking, and the silica particles were bound to the fibroin, resulting in improved thermal properties in differential scanning calorimetry patterns compared with SF [64].

Montmorillonite (MMT) clay is one of the most used for preparation of polymer nanocomposites. Polymer-MMT nanocomposites are known to have high strength, thermal properties and barrier properties for gases [61]. On the other hand, MMT has

been recently used in bone tissue engineering, because MMT is a biocompatible, bio-active and osteoinductive inorganic mineral with large surface area to volume [64, 65]. Mieszawska et al. [65] fabricated SF-MMT composite film by casting method. They reported that the SF-MMT composite film supported the attachment, proliferation and osteogenic differentiation of human bone marrow derived mesenchymal stem cells (hMSCs). Therefore, the electrospun SF nanofiber non-woven fabric-MMT composite material is expected to be a candidate for the producing new composite materials for tissue engineering like bone regeneration due to its biocompatibility, osteoinductivity and large surface area to volume.

## 5. Technical issues in preparation conditions of SF spinning solution for electrospinning

Electrospun SF nanofiber non-woven fabrics are used in various fields such as biomedical applications. However, harsh solvents have been employed on the electrospinning of SF such as formic acid, HFIP, HFA and trifluoroacetic acid. Jin et al. [44] firstly reported that the electrospinning of SF aqueous solution with poly-(ethylene oxide) (PEO) with high molecular weight (900,000g/mol) and attained uniform nanofibers but this technique involved the use of PEO which might have affected the mechanical properties and biocompatibility of SF nanofiber non-woven fabric. And, a complicated process to remove the PEO after electrospinning is required. However, it will be difficult to confirm the lack of existence of residual PEO in the SF nanofibers. To solve these problems, researches [39-43] have successfully fabricated SF nanofiber non-woven fabrics from only SF aqueous solution of *Bombyx mori* silk fibroin. They electrospun to produce nanofiber fabric using concentrated SF aqueous solution (17wt% <). Such high concentrations are disadvantageous for industrial processing because high

concentrated SF aqueous solution transform into gel easily than low concentration by interactions including hydrophobic interactions and hydrogen bonds [66]. Therefore, the electrospinning of SF aqueous solution at low concentration is ideal process for preparation of SF nanofiber non-woven fabrics.

On the other hand, reinforcement of electrospun SF nanofiber non-woven fabrics have been studied because its mechanical properties is low. Kim et al. [67] and Pan et al. [68] fabricated SF/hydroxyapatite nanoparticles composite nanofiber non-woven fabric and SF/carbon nanotube composite nanofiber non-woven fabrics respectively. They reported that the tensile strength of electrospun SF nanofiber non-woven fabrics were improved. Gandhi et al. [69], Ayutsede et al. [47] and Wei et al. [70] succeeded in enhancing the young modulus of electrospun SF nanofiber non-woven fabrics by incorporating of carbon nanotubes in SF spinning solutions. It is presumed that the poor mechanical properties of electrospun SF nanofiber non-woven fabric is caused by degradation of SF molecules during degumming process of cocoons [71, 72]. Theoretically, the mechanical properties of SF nanofiber non-woven fabric can be improved when the molecular weight of SF is higher, while lower limit concentration of SF aqueous solution for electrospinning will become lower.

## 6. Wet electrospun three dimensional nanofiber non-woven fabric

Many researches on an artificial scaffold have been focused on mimicking extracellular matrix (ECM) structure and various techniques to fabricate such a scaffold have been attempted. In generally, the freeze-drying and salt leaching methods are widely used because they are very simple to make the three dimensional porous structure [10, 18, 19, 73], but the structure is not similar to that of real natural ECM. The electrospun nanofiber fabric offers a highly porous structure as well as large surface area, a similar structural environment to the natural ECM to seeded cells [30]. However the size of pores and the porosity in the electrospun nanofiber fabric is very low due to the random deposition of nanofibers on the dry flat plate or rotating drum surface during the electrospinning. Such small pore size and low small porosity are not suitable for seeded cells to migrate into direction of thickness of nanofiber fabrics. Theoretically, three dimensional nanofiber fabric can be fabricated when the spinning time is increased. However, the porosity is still low even to increase the spinning time and the accumulation of the nanofibers have a limitation because the ability to continuously deposit nanofibers onto a three dimensional nanofiber fabric is hindered by the reduced conductivity of the grounded collector.

Yokoyama et al [74] and Ki et al [75, 76] have successfully developed a sponge like three dimensional nanofiber non-woven fabric using a modified electrospinning method (wet electrospinning). The wet electrospinning was equipped a liquid bath filled with poor solvent of spinning polymer instead of dry flat plate or rotating drum as a fiber collector. The relationship between solutions for the liquid bath in wet electrospinning and properties of the three dimensional non-woven fabric are summarized in table.3.
Ki et al. and Baek et al. [75-77] reported that the cell compatibility of wet electrospun

three dimensional SF fabric. As a results of cell adhesion and proliferation test of fibroblast cells, it was confirmed that the seeded cells were well proliferated in inner space of three dimensional SF nanofiber non-woven fabric because the structural features foam and its structural similarity ECM. However, they used formic acid and methanol as solvent of SF solution and liquid bath. Formic acid and methanol are harmful to living organisms and are hazardous during fabrication. These reagents are better to be avoided when producing medical materials such as cell scaffold. Therefore, fabrication of wet electrospun SF nanofiber non-woven fabric using SF aqueous solution and water based liquid bath is ideal processing for three dimensional tissue regeneration.

**Table.3** Preparation conditions of wet electrospinning and properties of wet electrospun nanofiber fabrics.

| Polymer | Solvent | Liquid bath | Pore size (μm) | Porosity (%) | Reference |
|---|---|---|---|---|---|
| PGA | HFIP | t-BuOH/water | | 85-96 | [74] |
| Silk fibroin | Formic acid | Methanol | 10-100 | <90 | [75] |
| Silk fibroin | Formic acid | Methanol with NaCl particles | 586-931 | 94±2 | [76] |
| Silk fibroin | Formic acid | Methanol with NaCl particles | 58-930 | 94±2 | [77] |
| Cellulose acetate | DMAc/DMSO 55/45 (v/v) | ethanol | 38-150 | 76-84 | [78] |

## 7. The purpose of study

In this study, I attempted to develop the SF nanofiber non-woven fabric scaffolds using electrospinning method for regenerative medical application with three major purpose.

First, development of new osteoinductive composite materials of SF nanofiber non-woven fabric and montmorillonite (MMT) for bone tissue engineering.

Second, development of electrospun SF nanofiber non-woven fabric using all SF aqueous solution at low concentration without water soluble polymer like PEO.

Third, development of three dimensional high porous SF nanofiber non-woven fabric using water based wet electrospinning technique for three dimensional tissue regeneration.

## 8. References


[1] C. Vepari, D.L. Kaplan, Silk as a Biomaterial, Prog. Polym. Sci., 32 (2007) 991-1007.

[2] W. Tao, M. Li, C. Zhao, Structure and properties of regenerated *Antheraea pernyi* silk fibroin in aqueous solution, Int. J. Biolo. Macromol., 40 (2007) 472-478.

[3] J. G. Hardy, L. M. Romer, T. R. Scheibel, Polymeric materials based on silk proteins, polymer, 49 (2008) 4309-4327.

[4] H. Wang, Y. Zhang, H. Shao, X. Hu, A study on the flow stability of regenerated silk fibroin aqueous solution, Int. J. Bio. Macromol., 36 (2005) 66-70.

[5] A. Ajisawa, Dissolution of silk fibroin with calcium chloride/ethanol aqueous solution, J. Seric. Sci. Jpn., 67 (1998) 91-94.

[6] Y. Goto, M. Tsukada, N. Minoura, Molecular cleavage of silk fibroin by an aqueous solution of lithium thiocynate, J. Seric. Sci. Jpn., 59 (1990) 402-409.

[7] N. Goujon, X. Wang, R. Rajkowa, N. Byrne, Regenerated silk fibroin using protic ionic liquids solvents: toward an all-ionic liquid process for producing silk with tunable properties, Chem. Commun., 48 (2012) 1278-1280.

[8] N. Minoura, M. Tsukada, M. Nagura, Fine structure and oxygen permeability of silk fibroin membrane treated with methanol, Polymer, 31 (1990) 265-269.

[9] U. J. Kim, J. Park, C. Li, H. J. Jin, R. Valluzzi, D. L. Kaplan, Structure and properties of silk hydrogels, Biomacromolecules, 5 (2004) 786-792.

[10] Y. Tamada, New process to Form a Silk Fibroin Porous 3-D Structure, Biomacromolecules, 6 (2005) 3100-3106.

[11] X. Zhang, M. R. Reagan, D. L. Kaplan, Electrospun silk biomaterial scaffolds for regenerative medicine, Adv. Drug. Deliv. Rev., 61 (2009) 988-1006.

[12] A. Sugihara, K. Sugiura, H. Morita, T. Ninagawa, K. Tubouchi, R. Tobe, M. Izumiya, T. Horio, N. Abraham, S. Ikehara, Promotive effects of a silk film on epidermal recovery from full-thickness skinwounds, Proc. Soc. Exp. Biol. Med., 225 (1) (2000) 58-64.

[13] V. Karageorgiou, L. Meinel, S. Hofmann, A. Malhotra, V. Volloch, D. L. Kaplan, Bone morphogenetic protein-2 decorated silk fibroin films induce osteogenic differentiation of human bone marrow stromal cells, J. Biomed. Mater. Res A., 71 (3) (2004) 528-537.

[14] S. Sofia, MB. McCarthy, G. Gronowicz, D. L. Kaplan, Functionalized silk-based biomaterials for bone formation, J. Biomed. Mater. Res., 54 (1) (2001)139-148.

[15] R .Kino, T. Ikoma, A. Monkawa, S. Yunoki, M. Munekata, J. Tanaka, T. Asakura, Deposition of bonelike apatite on modified silk fibroin films from simulated body fluid, J. Appl. Polym. Sci., 99 (5) (2006) 2822-2830.

[16] K. Hu, Q. Lv, F. Cui, Q. Feng, X. Kong, H. Wang, L. Huang, T. Li, Biocompatible fibroin blended films with recombinant human-like collagen for hepatic tissue engineering, J. Bioact. Compat. Polym., 21 (1) (2006) 23-37.

[17] K. Lee, S. Kong, W. Park, W. Ha, I. Kwon, Effect of surface properties on the antithrombogenicity of silk fibroin/S-carboxymethyl keratin blend films, J. Biomater. Sci Polym. Ed., 9 (9) (1998) 905-914.

[18] H. Aoki, N. Tomita, Y. Morita, K. Hattori, Y. Harada, M. Sonobe, S. Wakitani, Y. Tamada, Culture of chondrocytes in fibroin-hydrogel sponge, Biomed. Mater. Eng., 13 (4) (2003) 309-316.

[19] JH. Yeo, KG. Lee, HC. Kim, HYL. Oh, AJ. Kim, SY. Kim, The effects of PVA/chitosan/fibroin (PCF) 2- blended spongy sheets on wound healing in rats, Biol. Pharm. Bull., 23 (10) (2000) 1220-1223.

[20] L. Meinel, S. Hofmann, V. Karageorgiou, L. Zichner, R. Langer, D. L. Kaplan, G. Vunjak-Novakovic, Engineering cartilage-like tissue using human mesenchymal stem cells and silk protein scaffolds, Biotechnol. Bioeng., 88 (3) (2004) 379-391.

[21] Y. Wang, DJ. Blasioli, HJ. Kim, HS. Kim, D. L. Kaplan, Cartilage tissue engineering

with silk scaffolds and human articular chondrocytes, Biomaterials, 27 (25) (2006) 4434-4442.

[22] Y. Morita, N. Tomita, H. Aoki, S. Wakitani, Y. Tamada, T. Suguro, K. Ikeuchi, Visco-elastic properties of cartilage tissue regenerated with fibroin sponge, Biomed. Mater. Eng., (3) (2002) 291-298.

[23] Y. Morita, N. Tomita, H. Aoki, M. Sonobe, S. Wakitani, Y. Tamada, T. Suguro, K. Ikeuchi, Frictional properties of regenerated cartilage in vitro, J. Biomech., 39 (1) (2006) 103-109.

[24] S. Fuchs, A. Motta, C. Migliaresi, C. J. Kirkpatrick, Outgrowth endothelial cells isolated and expanded from human peripheral blood progenitor cells as a potential source of autologous cells for endothelialization of silk fibroin biomaterials, Biomaterials, 27 (31) (2006) 5399-5408.

[25] RE. Unger, K. Peters, M. Wolf, A. Motta, C. Migliaresi, CJ. Kirkpatrick, Endothelialization of a nonwoven silk fibroin net for use in tissue engineering: growth and gene regulation of human endothelial cells, Biomaterials, 25 (21) (2004), 5137-514.

[26] X. Tang, F. Ding, Y. Yang, N. Hu, H. Wu, X. Gu, Evaluation on in vitro biocompatibility of silk fibroin-based biomaterials with primarily cultured hippocampal neurons, J. Biomed. Mater. Res B. Appl. Biomater., 91 (2008) 166-174.

[27] T. Arai, G. Freddi, R. Innocenti, M. Tsukada, Biodegradation of Bombyx mori silk fibroin fibers and films, J. Appl. Polym. Sci., 91 (2004) 2383-2390.

[28] L. Meinel, S. S. Hofman, V. Karageorgiou, C. K. Head, J. McCool, G. Gronowicz, L. Zichnner, R. Langer, G. V. Novakovix, D. L. Kaplan, The inflammatory responses to silk films in vitro and in vivo, Biomaterials, 26 (2005) 147-155.

[29] H. Sakabe, H. Ito, T. Muyamoto, Y Noishiki, W. S. Ha, In vivo blood compatibility of regenerated silk fibroin, Seni`s gakkaishi., 45 (1989) 487-490.

[30] N. Bhardwaj, S. C. Kundu, Electrospinning: A fascinating fiber fabrication technique, Biotech. Adv., 28 (2010) 325-347.

[31] N. Kimura, H. Kim, B. Kim, K. Lee, I. Kim, Molecular Orientation and Crystalline Structure of Aligned Electrospun Nylon-6 Nanofibers; Effect of Gap Size, Macromol. Mater. Eng., 295, (2010) 1090-1096.

[32] X. Zhang, C. B. Baughman, D. L. Kaplan, In vitro evaluation of electrospun silk fibroin scaffolds for vascular cell growth, Biomaterials, 29 (2008) 2217-2227.

[33] C. Wong, S. V. Patwardhan, D. J. Belton, B. Kitchel, D. Anastasiades, J. Huang, R. R. Nalk, C. C Perry, D. L. Kaplan, Novel nanocomposites from spider silk-silica fusion (chimeric) proteins, PNAS, 103 ( 2006) 9428-9433.

[34] K. Ohgo, C. Zhao, M, Kobayashi, T. Asakura, Preparation of non-woven nanofibers of Bombyx mori silk, *Samia cythia ricini* silk and recombinant hybrid silk with electrospinning method, Polymer, 44 (2003) 841-846.

[35] X. Zhang, M. M. R. Khan, T. Yamamoto, M. Tsukada, H. Morikawa, Fabrication of silk sericin nanofibers from a silk sericin-hope cocoon with Electrospinning method.,Int J Bio Macrom., 50 (2012) 337-347.

[36] X. Zhang, K. Aojima, M. Miura, M. Tsukada, H. Morikawa, Fabrication of electrospun Tussah silk fibroin nanofibers, J Silk Sci. Tech. Jpn., 20 (2012) 61-67.

[37] X. Zhang, K. Aojima, M. Miura, M. Tsukada, H. Morikawa, Physical properties of electrospun Tussah silk fibroin nanofibers, J. Silk Sci. Tech. Jpn., 20 (2012) 69-76.

[38] X. Zhang, M. Tsukada, H. Morikawa, K. Aojima, G. Zhang, M. Miura, Production of silk sericin/silk fibroin blend nanofibers, Nanoscale Research Letters, 6 (2011) 510.

[39] H. Wang, Y. Zhang, H. Shao, X. Hu, Electrospun ultra-fine silk fibroin fibers from aqueous solutions, Journal of Materials Science, 40 (20) (2005) 5359-5363.

[40] H. Cao, X. Chen, L. Huang, Z. Shao, Electrospinning of reconstituted silk fiber from aqueous silk fibroin solution, Materials Science and Engineering: C, 29 (7) (2009) 2270-2274.

[41] B.-M. Min, L. Jeong, K.Y. Lee, W.H. Park, Regenerated Silk Fibroin Nanofibers:

Water Vapor-Induced Structural Changes and Their Effects on the Behavior of Normal Human Cells, Macromolecular Bioscience, 6 (4) (2006) 285–292.

[42] C. Chen, C. Chuanbao, M. Xilan, T. Yin, Z. Hesun, Preparation of non-woven mats from all-aqueous silk fibroin solution with electrospinning method, Polymer, 47 (18) (2006) 6322-6327.

[43] J. Zhu, H. Shao, X. Hu, Morphology and structure of electrospun mats from regenerated silk fibroin aqueous solutions with adjusting pH, Int. J. Biol. Macromol., 41 (4) (2007) 469-474.

[44] H-J. Jin, S.V. Fridrik, G.C. Rutledge, D.L. Kaplan, Electrospinning *Bombyx mori* Silk with Poly (ethylene oxide), Biomacromolecules, 3 (2002) 1233-1239.

[45] S. Fan, Y. Zhang, H. Shao, X. Hu, Electrospun regenerated silk fibroin with enhanced mechanical properties, Int. J. Biol. Macromol., 56 (2013) 83-88.

[46] S. Putthanarat, R. K. Eby, W. Kataphinan, S. Jones, R. Naik, D.H. Reneker, B.L. Farmer, Electrospun Bombyx mori gland silk, Polymer, 47 (2006) 5630-5632.

[47] J. Ayutsede, M. Gandhi, S. Sukigara, H. Ye, C. Hsu, Y. Gogotsi, F. Ko, Carbon Nanotube Reinforced Bombyx mori Silk Nanofibers by the Electrospinning Process, Biomacromolecules, 7 (2006) 208-214.

[48] J. Huang, L. Liu, J. Yao, Electrospinning of Bombyx mori Silk Fibroin Nanofiber Mats Reinforced by Cellulose Nanowhiskers, Fibers and Polymers, 12 (8) (2011) 1002-1006.

[49] N. Amiraliyan, M. Nouri, M. H. Kish, Structural Characterization and Mechanical Properties of Electrospun Silk Fibroin Nanofiber Mats[1], Polymer Science, Ser. A., 52 (4) (2010) 407-412.

[50] S. D. Aznar-Cervantes, D.Viecente-Cervantes, L. Meseguer-Olmo, J. L. Cenis, A. Lozano-Perez, Influence of the protocol used for fibroin extraction on the mechanical properties and fiber sizes of electrospun silk mats, Mater. Sci. Eng. C., 33 (2013) 1945-1950.

[51] J. He, N. Guo, S. Cui, Structure and Mechanical Properties of Electrospun Tussah Silk Fibroin Nanofibres: Variations in Processing Parameters, Iranian. polym. J., 20 (9) (2011) 713-724.

[52] B. M. Min, L. Jeong, K. Y. Lee, W. H. Park, Regenerated Silk Fibroin Nanofibers: Water Vapor-Induced Structural Changes and Their Effects in the Behavior of Normal Human Cells, Macromolecular bioscience, 6 (2006) 285-292.

[53] H. J. Jin, J. Chen, V. Karageorgiou, G. H. Altman, D. L. Kaplan, Human bone marrow stromal cell responses on electrospun silk fibroin mats, Biomaterials, 25 (2004) 1039-1047.

[54] X. Huang, S. Fan, A. I. M. Altayp, Y. Zhang, H. Shao, X. Hu, M. Xie, Y. Xu, Tunable Structures and Properties of Electrospun Regenerated Silk Fibroin Mats Annealed in Water Vapor at Different Times and Temperatures, J. Nanomater., 7 (2014).

[55] H. Cao, X. Chen, L. Huang, Z. Shao, Electrospinning of reconstituted silk fiber from aqueous silk fibroin solution, Mater. Sci. Eng. C., 29 (2009) 2270-2274.

[56] S. Zarkoob, D.H. Reneker, R. K. Eby, S. D. Hudson, D. Ertley, W. W. Adams, Structure and morphology of regenerated silk nano-fibers produced by electrospinning, Polym. Preprints., 39 (1998) 244-245.

[57] S. Sukigara, M. Gandhi. J. Ayutsede, M. Miklus, F. Ko, Regeneration of Bombyx mori Silk by electrospinning process- Part 1: Processing Parameter and Geometric Properties, Polymer, 44 (19) (2003) 5721-5727.

[58] S. Sukigara, M. Gandhi. J. Ayutsede, M. Miklus, F. Ko, Regeneration of Bombyx mori Silk by electrospinning process-Part 2: Process Optimization, Polymer, 45 (11) (2004) 3701-3708.

[59] J. Ayutsede, M. Grandhi, S. Sukigara, M. Miklus, H. Chen, F. Ko, Regeneration of Electrospun Non-woven Mat, Polymer, 46 (5) (2005) 1625-1634.

[60] A.Matsumoto, J. Chen, A.L. Collette, U.J. Kim, G.H. Altman, P. Cebe, D.L. Kaplan, Mechanism of silk fibroin sol-gel transitions, J. Phys. Chem. B., 110 (2006) 21630-21638.

[61] H. Kim, L. Che, Y. Ha, W. Ryu, Mechanically-reinforced electrospun composite silk fibroin nanofibers containing hydroxyapatite nanoparticles, Materials Science and Engineering C, 40 (2014) 324-335.

[62] H. Pan, Y. Zhang, Y. Hang, H Shao, X. Hu, Y. Xu, C. Feng, Significantly Reinforced Composite Fibers Electrospun from Silk Fibroin/Carbone Nanotube Aqueous Solution, Macromolecules, 13 (2012), 2859-2867.

[63] M. Gandhi, H. Yang, L. Shor, F. Ko, Post-spinning modification of electrospun nanofiber nanocomposite from Bombyx mori silk and carbon nanotubes, Polymer, 8 (9) (2009) 1918-1924.

[64] K. Wei, J-H. Xia, B-S. Kim, I-S. Kim, Multiwalled carbon nanotubes incorporated Bombyx mori silk nanofibers by electrospinning, Journal of Polymer Research, 18 (4) (2011) 579-585.

[65] K. Yoon, H. N. Lee, C. S. Ki, D. Fang, E.S. Hsiao, B. Chu, I.C. Um, Effects of degumming consitions on electrospinning rate of regenerated silk, Int. J. Biolo. Macromol., 61 (2013) 50-57.

[66] J. S. Ko, K. Yoon, C. S. Ki, H. J. Kim, D. G. Bae, K. K. Lee, Y. H. Park, I. C. Um, Effects of degumming conditions on the solution properties and electrospinning of regenerated silk solution, Int. J. Biolo. Macromol., 55 (2013) 161-168.

[67] R. Nazarov, H. J. Jin, D. L. Kaplan, Porous 3-D Scaffolds from Regenerated Silk Fibroin, Biomacromolecules, 5 (2004) 718-726.

[68] Y. Yokoyama, S. Hattori, C. Yoshikawa, Y. Tasuda, H Koyama, T Takao, H. Kobayashi, Novel wet electrospinning system for fabrication of spongiform nanofiber 3-dimensional fabric, Materials letter, 63 (2009) 754-756.

[69] C. S. Ki, J. W. Kim, J. H. Hyun, K. H. Lee, M. Hattori, D. K. Rah, Y. H. Park, Electrospun Three-Dimensional Silk Fibroin Nanofibrous Scaffold, J. App. Polym. Sci., 106 (2007) 3922-3928.

[70] C. S. Ki, S. Y. Park, H. J. Kim, H. M. Jung, K. M. Woo, J. W. Lee, Y. H. Park,

Development of 3-D nanofibrous fibroin scaffold with high porosity by electrospinning: implications for bone regeneration, Biotechnol. Lett., 30 (2008) 405-410.

[71] H. S. Baek, Y. H. Park, C. E. Ki, J. C. Park, D. K. Rah, Enhanced chondrogenic responses of articular chondrocytes onto porous silk fibroin scaffolds treated with microwave-induced argon plasma, Surface & Coatings Technology, 202 (2008) 5794-5797.

[72] D. Atilla, D. Keskin, A. Tezcaner, Cellulose acetate based 3-dimensional electrospun scaffold for skin tissue engineering applications, Carbohydrate Polymers, 133 (8) (2015) 251-261.

[73] A. R. Allafi, M. A. Pascall, The effect of different percent loadings of nanoparticles on the barrier and thermal properties of nylon 6 films, Innovative Food Science & Emerging Technologies, 20 (2013) 276-280.

[74] M. J. Dumont, A. R. Valencia, J. P. Emond, M. Bousmina, Barrier properties of polypropylene/organoclay nanocomposites, Journal of Applied Polymer Science, 103 (2007) 618-625.

[75] J. Han, Y. Dou, D. Yan, J. Ma, M. Wei, D.G. Evans, X. Duan, biomimetic design and assembly of organic-inorganic composite films with simultaneously enhanced strength and toughness, Chemical Communications, 47 (2011) 5274-5276.

[76] A.J. Mieszawska, N. Fourligas, I. Georgakoudi, N.M. Ouhib, D.J. Belton, C.C. Perry, D.L. Kaplan, Osteoinductive silk-silica composite biomaterials for bone regeneration, Biomaterials, 31 (2010) 8902–8910.

[77] A. Hou, H. Chen, Preparation and characterization of silk/silica hybrid biomaterials by sol-gel crosslinking process, Materials Science and Engineering: B, 167 (2010) 124-128.

[78] A.J. Mieszawska, J. G. Llamas, C. A. Vaiana, M. P. Kadakia, R. R. Naik, D.L. Kaplan, Clay-Enriched Silk Biomaterials for Bone Formation, Acta. Biomaterial., 7 (8) (2011) 3036-3041.

# Chapter 2: Nanocomposite of silk fibroin nanofiber and montmorillonite: Fabrication and morphology

## Chapter 2: Nanocomposite of silk fibroin nanofiber and montmorillonite: Fabrication and morphology


### Abstract

The purpose of our research is creating a new nanocomposite material. Generally silk fibroin (SF) is regarded as a promising base material for biomedical uses. The incorporation of montmorillonite (MMT) into SF fibers would improve physical properties of the SF fibers. We investigated a new method of combining electospun SF with MMT. Specifically, electrospun silk nanofibers were treated with methanol and dipped in a MMT suspension. We could obtain a nanosheet composite of silk nanofibers and MMT. Their ultrastructures were successfully visualized by high resolution transmission electron microscopy. This compound was comprised of individual silk nanofibers surrounded by thin layers of MMT, each with a thickness of about 1.2 nm. This structure was confirmed by elemental analysis. We also performed IR, NMR and X-ray diffraction analyses in conjunction with morphological data. Conclusively we obtained a new composite of silk nanofiber and MMT, which has never been reported. Using this unique nanocomposite biological tests of its application for a scaffold for tissue engineering are under way.

## 1. Introduction

Silk fibroin (SF) has attracted significant attention in the development of new materials, because SF is a biodegradable and biocompatible natural polymer with a high chemical reactivity and excellent mechanical properties [1]. SF can be electrospun to fabricate a non-woven sheet composed of nanoscale fibers. Therefore, electrospun SF is expected to be a candidate for the manufacturing new organic/inorganic nanohybrid materials with advanced structures and properties.

In recent years, nanomaterials have gained considerable attention because they exhibit properties that are significantly different to the corresponding bulk materials, such as large surface area, high strength, and enhanced surface reactivity [2]. In this study, we combined electrospun SF with a silica compound of montmorillonite (MMT) clay to produce silk/silica materials. Other silk/silica particles were reportedly produced by combining SF with silica particles, and have been used as an osteoinductive composite for bone generation [3]. Another silk/silica complex was prepared by sol–gel crosslinking, and the silica particles were bound to the fibroin, resulting in improved thermal properties in differential scanning calorimetry patterns compared with SF [4].

This communication deals with our research in creating new nanoSF/MMT composites by use of a simple method. The product had an interesting nanostructure, in which the SF nanofibers and thin MMT were combined in a unique way. We investigated this nanostructure by high-

resolution transmission electron microscopy (TEM). We also performed IR, NMR and X-ray diffraction analyses in conjunction with morphological data.

This nanocomposite is a candidate for new biocompatible application as scaffold for tissue engineering like bone regeneration, because the composite contains biodegradable silk and osteoinductive MMT [3] and moreover the composite nanofiber may be advantageous scaffold in cell culture due to high surface area [5].

## 2. Materials and methods

### 2.1. Materials

Cocoons of Bombyx mori silkworm silk were used for the preparation of SF nanofiber. SF was extracted from silk composed of fibroin and sericine, according to a previously described method [6]. The cocoons were sliced into four pieces and suspended in a boiling 2.5 (w/v) % sodium carbonate solution for 30 min to obtain scoured cocoons, which were then washed in running tap water for two days. The washed specimens were air-dried, and then further dried in an oven at 105 °C for 90 min. SF fibers were dissolved in a 9 M lithium bromide solution at 55–60 °C, and then dialyzed through a cellulose membrane against distilled water. The aqueous fibroin solution was freeze-dried to give dry SF powder (regenerated SF). The montmorillonite (MMT) used was purchased from Kunimine industries Co. Ltd., Japan (Kunipia F). MMT clay is one of the most commonly used layered silicates, with the formula Si8 (Al3.34 Mg0.66) Na0.66 (OH)4 and a crystal lattice of octahedral sheets [7].

### 2.2. Electrospinning of SF nanofiber

Silk fibroin (SF) was dissolved in trifluoro acetic acid (TFA) to form a uniform polymer solution. The solution was stirred at room temperature for 3 h. The concentrations of silk/TFA solution were 8, 10 and 12 wt%. An

electrospinning apparatus manufactured by Kato Tech Company (Kyoto, Japan) was used, and was operated at room temperature. The silk/TFA solution was placed into 5 mL syringe (SS-01T, Terumo Corporation, Tokyo, Japan) with a 21 gauge stainless needle (NN-2238N, Terumo Corporation, Tokyo, Japan), which connected the high voltage power supply. The procedure used was in basic accordance with that described in a previous paper [8] dealing with the fabrication of silk sericine nanofibers in our laboratory. During electrospinning, an electric voltage (20–30 kV) was applied to droplets of SF/TFA solution. The electrospun nanofibers were collected on wax paper, which was placed at a distance of 15 cm from the syringe.

### 2.3. Fabrication of nanoSF/MMT composite

To form a composite of SF nanofibers and MMT, SF nanofibers were immersed in pure methanol (WAKO Ltd.) for 15 min, and were then dried at room temperature for 24 h. Through methanol treatment, the SF nanofibers were transformed from a random coil structure into a β-sheet conformation [9]. The SF nanofibers were dipped in an MMT aqueous suspension at concentrations of 0.1, 0.5 and 1 wt%, and the products were dried at room temperature for 12 h to produce nanoSF/MMT composites.

## 2.4. Characterization

The morphology of the electrospun SF nanofiber was observed with a scanning electron microscope (SEM: JSM-6010LA; JEOL Ltd., Tokyo, Japan) at 10 kv after sputter-coating with platinum. And the morphology of the nanoSF/MMT composite was observed using field emission SEM (FESEM: SU8000 and SU8040; Hitachi HTA, Inc., Tokyo, Japan) at 20 kV and 0.8 kV. Cross-sectional samples were Ar-ion milled using a Hitachi IM400 and sputter-coated with platinum. Transmission electron microscopy (TEM: JEM-2100F, JEOL Ltd., Tokyo, Japan) was used to observe the detailed structure of the nanoSF/MMT composite. To characterize the fine structure of the nanoSF/MMT composite, samples were observed by high resolution TEM (JEM-2800; JEOL Ltd., Tokyo, Japan) at 200 kv and analyzed in detail using EDS. The EDS data were collected using a JEOL JED-2300T EDS system combined with a JEOL JEM-2100F microscope. The bulk material was embedded in the resin and then thin sections were cut using a Leica Ultracut UCT.

Fourier transform infrared (FTIR) spectroscopy was performed using a Shimadzu FTIR, IR Prestige-21 infrared spectrometer and the ATR method (attenuated total reflectance) in the region of 4000–500 $cm^{-1}$ at room temperature.

X-ray diffraction patterns of the samples were measured with an X-ray diffractometer (Rigaku Denki Corporation, Japan), using Cu Kα radiation at 40 kV, 150 mA, and $\lambda = 0.1542$ nm.

## 3. Results and discussion

### 3.1. Effect of the concentration of SF/TFA solution and applied voltage

The SF nanofiber morphology was strongly influenced by the electrospinning conditions [9]. In electrospinning processes, the concentration of the polymer solution and the applied voltage are important factors. Fig. 1 shows SEM images of a specimen produced using an applied voltage of 20 kV. When the concentration of SF/TFA was 8 wt%, beads occasionally appeared (Fig. 1(a)) in the mat. On the other hand, for a 10 and 12 wt% SF/TFA solution, a homogeneous structure without beads was observed (Fig. 1(b) and (c)).

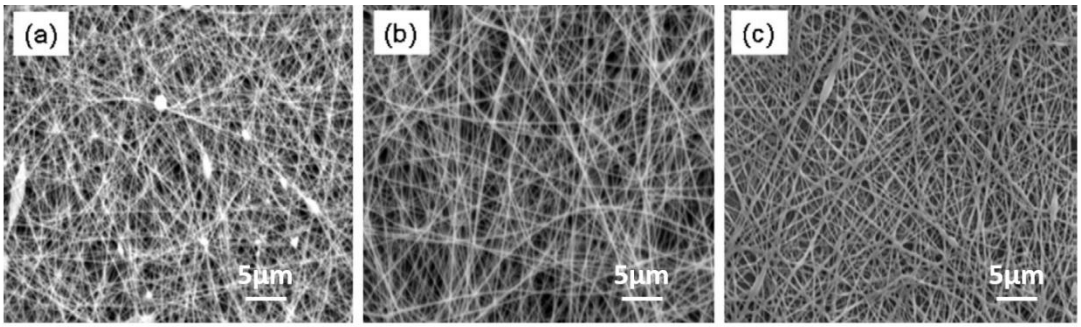


**Fig. 1.** SEM images of non-woven silk nanofibers formed at a voltage of 20 kV and solution concentrations of (a) 8 wt%, (b) 10 wt% and (c) 12 wt%.

The beads probably disappeared because the jet was stabilized by surface tension in the presence of adequate electrical forces [2]. Beads were also absent when the applied voltage was increased to 30 kV (data not shown). At 20 kV, SF/TFA solution concentrations of 8, 10 and 12 wt% yielded average SF fiber diameters of 118, 214 and 399 nm, respectively. In the present study, we produced fibers using a 10 wt% SF/TFA solution under a 20 kV bias, which gave fine fibers about 200 nm in diameter, and no bead formation was observed (Fig. 1(b)).

### 3.2. FT-IR spectra of methanol treated SF nanofiber

Through methanol treatment, the SF nanofibers were transformed from a random coil structure into a β-sheet conformation [9]. Fourier transform infrared (FT-IR, IR Prestige-21; Shimadzu, Ltd., Tokyo, Japan) spectroscopy was applied to determine the molecular conformation of the SF nanofibers (Fig. 2). The FT-IR spectra confirmed the transformation of silk fibroin from a random coil structure to a β-sheet conformation in the amide I and II regions. The as-spun SF nanofiber had absorption bands at 1651 $cm^{-1}$ (amid I) and 1528 $cm^{-1}$ (amid II), which were attributed to a random coil. On the other hand, the methanol treated SF nanofiber showed bands associated with the β-sheet conformation at 1623 $cm^{-1}$(amid I) and 1515 $cm^{-1}$ (amid II) [9]. By methanol treatment, SF nanofiber was insolubilized in water.

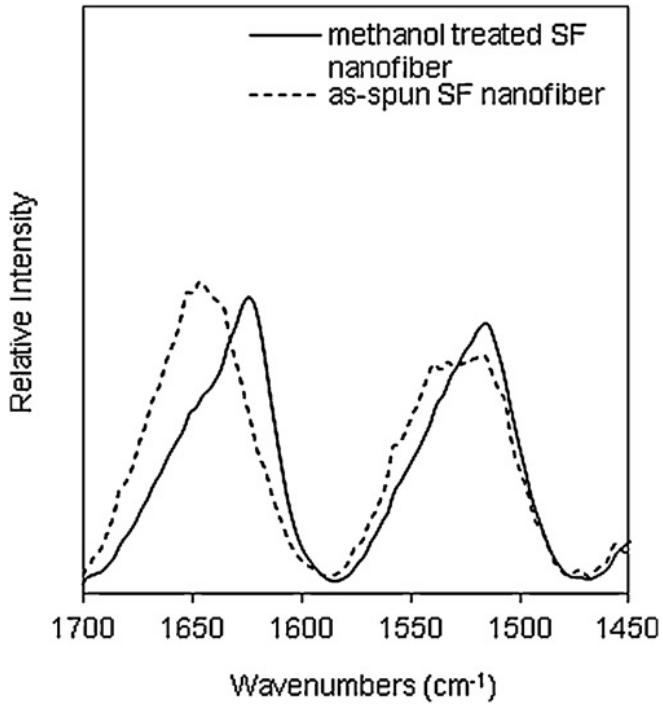


**Fig. 2.** FT-IR spectra of the methanol treated SF nanofiber (solid line) and as-spun SF nanofiber (dashed line).

### 3.3. Preparation of nanoSF/MMT composite

For preparation of nanoSF/MMT composites, the MMT suspension was spread on a sheet of electrospun SF nanofiber. The products obtained, however, had irregular surfaces. Alternately we tried dipping of the SF nanofiber in an MMT aqueous suspension at 0.1, 0.5 and 1%, and the products were dried at room temperature for 12 h to produce nanoSF/MMT composites. Fig. 3(a) shows that the obtained film containing SF nanofibers that were apparently bonded to the MMT. Here, the concentration of the MMT aqueous suspension was 0.5 wt%, but at 0.1 and 1 wt%, the products were basically the same (data not shown). By comparison with Fig. 1, it is clear that the morphology of the nanofibers was unaltered. The nanoSF/MMT composites in sheet form were sliced for cross-sectional viewing (Fig. 3(b)). The fibrous structures of the nanoSF/MMT composites were found to be intermingled in a sheet about 2.5 μm thick. Individual nanofibers showed a circular cross-section.

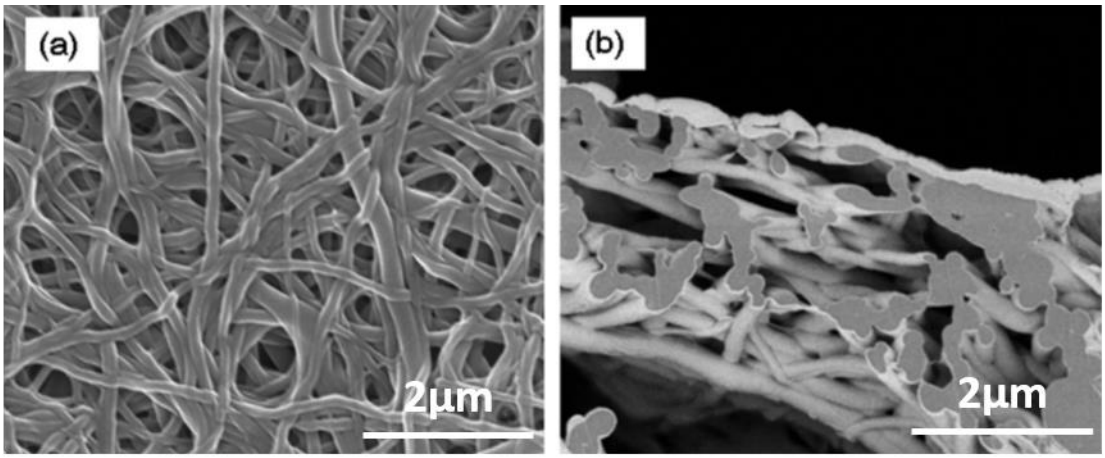


**Fig.3.** FESEM images of nanoSF/MMT composites. The MMT aqueous suspension concentration was 0.5 wt%.

### 3.4. TEM morphology of the nanoSF/MMT composite

TEM was used to observe the detailed structure of this specimen (Fig. 4). As indicated by the circle, thin membranes, which were shown to be MMT by energy dispersive spectroscopic (EDS) analysis, and were present between the SF nanofibers.

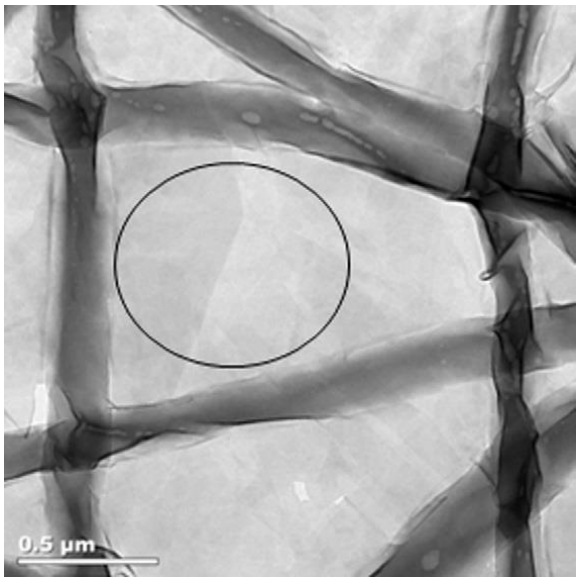


**Fig. 4.** TEM images of nanoSF/MMT composites at 10,000× magnification.

From the TEM images shown in Fig. 5, individual SF nanofibers were surrounded by a thin MMT layer. Fig. 5(a) shows a TEM image of a cross section of a nanofiber. It can be seen that it is not a perfect circle, but is distorted, probably as an artifact of the slicing process. In Fig. 5(b), at a magnification of 200 K, a layered architecture is observed. To confirm the presence of MMT, TEM-EDS mapping was carried out, as shown in Fig. 5(c)–(g). The EDS mapping results indicated that O, Al, Si and Mg atoms, which

are constituent elements of MMT, were distributed on the surface of the SF nanofiber. Therefore, nanoSF/MMT composites were successfully synthesized via dipping in an MMT suspension.

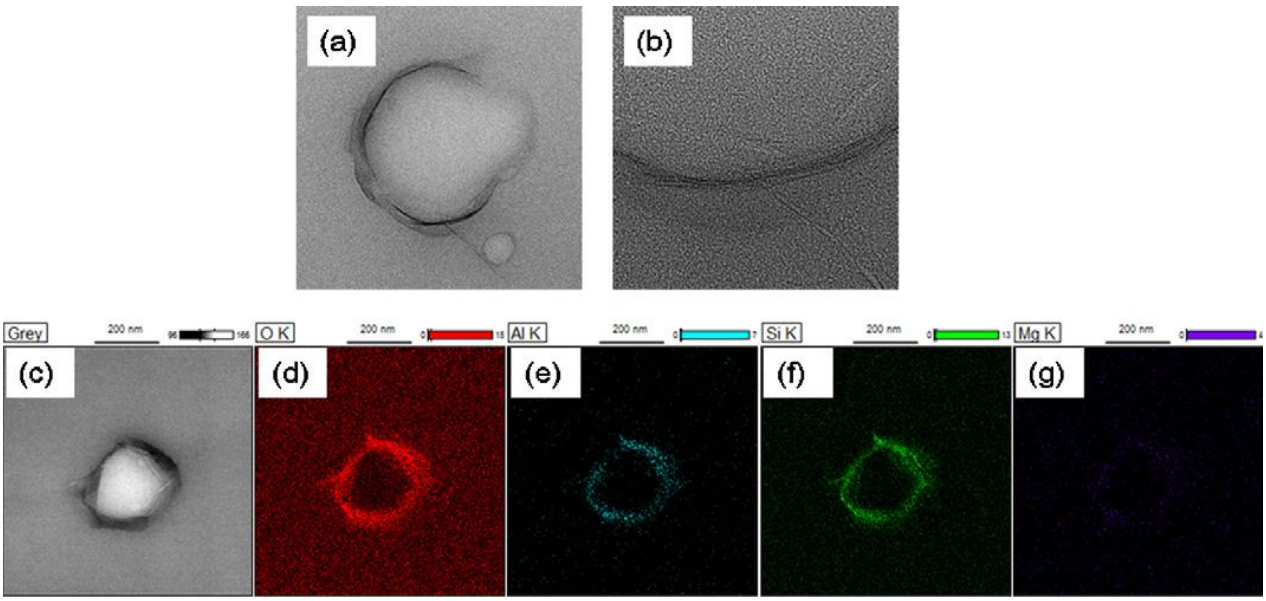


**Fig. 5.** Cross-sectional TEM images and energy dispersive spectroscopy (EDS) maps of silk nanofiber/MMT nanocomposites. (a) 50,000× magnification and (b) 200,000× magnification. (c)–(g) show EDS mapping data for oxygen, aluminum, silicon, and magnesium, respectively, for the region shown in (c).

The above results clearly revealed the detailed morphology of these nanoSF/MMT composites. This is the first successful creation of a new composite in which SF nanofibers are surrounded by thin layers of MMT, each with a thickness of approximately 1.2 nm.

### 3.5. FTIR ATR, NMR and XRD analyses of the nanoSF/MMT composites

FTIR ATR profiles of SF nanofibers, pristine MMT and nanoSF/MMT composites indicated no chemical interaction between SF nanofiber and MMT in the composite formation (FTIR ATR is shown in Fig. S1 in Supplementary Data). Solid-state 13C NMR spectroscopies of SF nanofiber and pristine MMT provided the same pattern, indicating MMT did not react with SF nanofiber as shown in Fig. S3 in Supplementary Data.

Fig. 6 displays XRD patterns of pristine MMT and nanoSF/MMT composites. The pristine MMT clay generated primary peak at $2\theta = 6.8°$. According to Bragg equation, the spacing of the pristine MMT was calculated to be 1.3 nm. In the composite, this peak shifted to 5.4°, corresponding to a spacing of 1.6 nm, which is broader than that of pristine MMT.

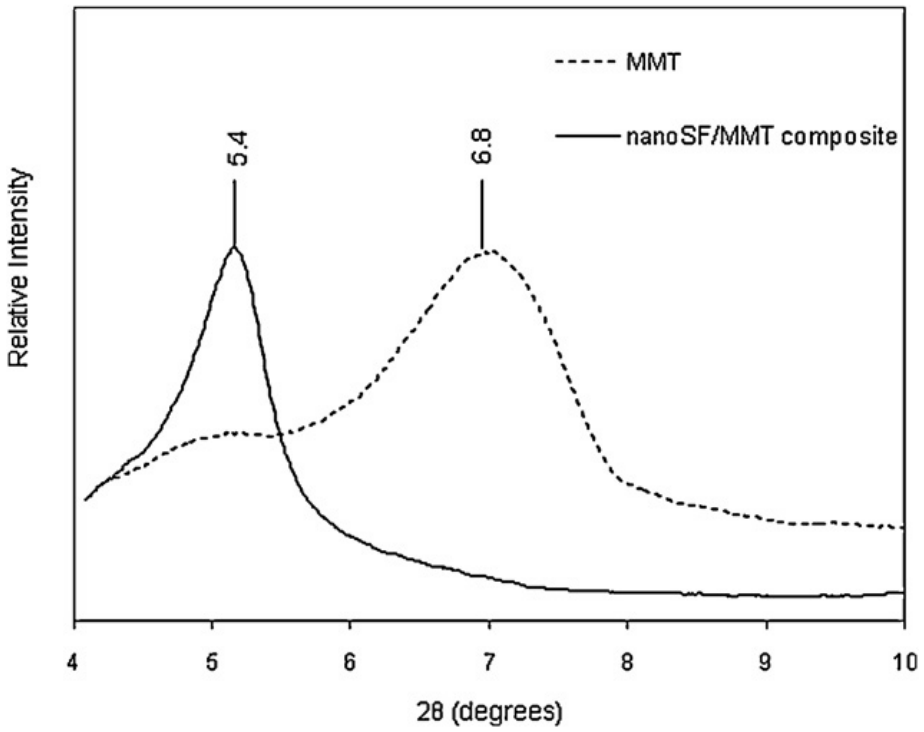


**Fig. 6.** XRD patterns of pristine MMT (dashdotted line) and nanoSF/MMT composite (continuous line).

Previously reported silk/MMT clay and silk/clay composites were MMTs dispersed in silk protein [10] or silica particles incorporated into silk films or bound to SF [3] and [4]. These are quite different from the above mentioned novel nanoSF/MMT composites. Their ultrastructures were successfully visualized by high resolution transmission electron microscopy. This compound was comprised of individual silk nanofibers surrounded by thin layers of MMT, each with a thickness of about 1.2 nm. This material is unique in that each SF nanofiber is surrounded or protected by MMT layers. It is very likely that the surface charge of the silk was altered by covering it with a thin layer of MMT. Using this unique nanocomposite biological tests of its application for a scaffold for tissue engineering are under way.

## 4. References

[1] C. Vepari, D.L. Kaplan, Progress in Polymer Science 32 (2007) 991–1007.

[2] N. Bhardwaj, S.C. Kundu, Biotechnology Advances 28 (2010) 325–347.

[3] A.J. Mieszawska, N. Fourligas, I. Georgakoudi, N.M. Ouhib, D.J. Belton, C.C. Perry, D.L. Kaplan, Biomaterials 31 (2010) 8902–8910.

[4] A. Hou, H. Chen, Materials Science and Engineering: B 167 (2010) 124–128.

[5] Y.Z. Zhang, B. Su, J. Venugopal, S. Ramakrishna, C.T. Lim, International Journal of Nanomedicine 2 (4) (2007) 623–638.

[6] C. Chen, C. Chuanbao, M. Xilan, T. Yin, Z. Hesun, Polymer 47 (2006) 6322–6327.

[7] A.J. Mieszawska, J.G. Llamas, C.A. Vaiana, M.P. Kadakia, R.R. Naik, D.L. Kaplan, Acta Biomaterialia 7 (2011) 3036–3041.

[8] X. Zhang, M.M.R. Khan, T. Yamamoto, M. Tsukada, H. Morikawa, International Journal of Biological Macromolecules 50 (2012) 337–347.

[9] S.H. Kim, Y.S. Nam, T.S. Lee, W.H. Park, Polymer Journal 35 (2003) 185–190.

[10] Q. Dang, S. Lu, S. Yu, P. Sun, Z. Yuan, Biomacromolecules 11 (2010) 1796–1801.

# Chapter 3: Electrospinning of silk fibroin from all aqueous solution at low concentration

## Chapter 3: Electrospinning of silk fibroin from all aqueous solution at low concentration


### Abstract

Non-woven mats of Bombyx mori silk fibroin were fabricated using electrospinning with an all aqueous solution at < 10 wt% without any co-existing water soluble polymer such as PEO. The fibroin aqueous solution electrospinnability was affected by the fibroin molecular weight and the spinning solution pH. Hot-water treatment without any alkaline reagent or soap produced higher molecular weight fibroin than the typical degumming process did. The higher molecular weight fibroin provided good electrospinnability. Results show that the basic solution (pH 10–11) is important for electrospinning at low concentrations of 5 wt%. Evaluation of structural and mechanical properties of the non-woven mat fabricated with water solvent revealed that it is safe for use in the human body. It is anticipated for wider use in medical materials such as cellular scaffolds for tissue engineering.

## 1. Introduction

Silk applications have been expanding beyond textile use [1] and [2]. Especially, studies of silk-based materials intended for use as biomaterials used in medical applications have attracted a great deal of attention [3] and [4]. This interest is attributable to the biocompatibility and mechanical advantages of silk, supported by its > 2500 years of use for surgical sutures [5]. Moreover, silk fibroin (SF) can be fabricated to various forms such as films, gels, resins, and sponges [6]. Recently electrospun non-woven mats consisting of fine fibers from tens of nanometers to a few micrometers in diameter have been specifically examined for the development of cell scaffolds in tissue engineering [7]. SF is also used as the spinning solution for electrospinning to produce non-woven mats. Sukigara et al. [8] reported electrospinning of Bombyx mori SF in a formic acid solvent and indicated SF concentration as the most important parameter when spinning uniform and cylindrical fibers of < 100 nm in diameter by controlling various parameters. Zhang et al. [9] fabricated SF nanofibers of 50–300 nm diameter using a SF nanofilament solution in formic acid from < 10 wt% concentration. Ohgo et al. [10] demonstrated that the concentration of silk fibroins in hexafluoroacetone (HFA) affected the fiber diameter in a non-woven mat formed by electrospinning. Zarkoob et al. [11] presented structures and morphologies of SF nanofibers that had been electrospun from hexafluoro isopropanol (HFIP).

One expected application of the electrospun SF non-woven mats is for cellular scaffolds in regenerative medicine [12] and [13]. For medical use, the

materials must be safe for cells and living human bodies. Silk's benefits for safety naturally derive from both the material itself and its fabrication processes. Regarding SF scaffolds, SF has been widely reported as safe and biocompatible [14]. Therefore, the security of scaffold safety will depend on the solvents and chemical reagents used for fabrication. To prevent risks from residual solvents in the scaffold, solvents used for electrospinning must not be harmful to cells or the human body. The safest solvent for the human body is water. Therefore, several studies have examined the formation of non-woven mats by electrospinning from an aqueous SF solution. Wang et al. [15] fabricated electrospun nanofibers from an all aqueous SF solution. They reported that fibers of 400–800 nm diameter were electrospun with 28 w/v% solution, but fibers did not form at < 17% solution. Such high concentrations are disadvantageous for industrial processing because high concentrated SF aqueous solution transform into gel easily than low concentration by interactions including hydrophobic interactions and hydrogen bonds [16]. Jin et al. [17] developed a poly (ethylene oxide) (PEO) blending technique for electrospinning from a low SF aqueous solution (3–7.2 wt/v%) to overcome the problem in the SF aqueous process. SF fibers with diameters of around 800 nm were observed using this PEO blending technique [18]. However, a complicated process to remove the PEO after spinning is required. It will be difficult to confirm the completely absence of the residual PEO in the non-woven mat. Furthermore, the influence of the residual PEO on cell adhesion and proliferation was reported [19].

For this study, we attempted to develop a SF non-woven mat using

electrospinning technique with all SF aqueous solutions at low concentration with no other blending polymer. To achieve that goal, we reconsidered the degumming process and the spinning solution conditions with emphasis on pH. Furthermore, the resulting SF non-woven mats were analyzed to ascertain their structure and mechanical properties.

## 2. Materials and methods

### 2.1. Materials

*Bombyx mori* silkworm cocoons were generously provided by the experimental farm at Shinshu University. Chemical reagents, sodium carbonate (Na2CO3), lithium bromide (LiBr), ethanol, methanol, 5 M sodium hydroxide (NaOH) solution, and polyethylene glycol (PEG, Mw; 20,000 ± 5000 Da) were purchased from Wako Pure Chemical Inds. Ltd. (Tokyo, Japan) without further purification. Cellulose dialysis membrane tubes (molecular weight cut off: 12,000–14,000 Da) were purchased from Kenis Ltd. (Tokyo, Japan).

### 2.2. Degumming and SF aqueous solution preparation

Two degumming processes were used to prepare a silk fibroin (SF) aqueous solution. According to the typical degumming process reported in the literature [13], cocoons were boiled in 0.5 or 2.5 w/v% of Na2CO3 solution for 30 min at 1:200 of the bath ratio. Then the degummed fibers were washed thoroughly in water. Another process is the boiling water process. Cocoons were boiled in water with no reagents for a predetermined duration (30–150 min) at the same bath ratio with Na2CO3 process, followed by washing in water by drawing the degummed fibers to strip off the sericin. The degummed SF fibers were dried for 1 day at room temperature. After cocoons were boiled

in the degumming solution to remove sericin, they were washed with hot water and dried at room temperature for 1 day. The dried SF fibers were weighted. The degumming ratio was calculated using the following equation.

$$degumming\ ratio = \frac{W_1 - W_2}{W_1} \times 100$$

Therein, W1 and W2 respectively denote the cocoon weight and degummed fiber weight. The sample code and degumming conditions are presented in Table 1.

**Table1.** Degumming process and degumming ratio.

| Sample code | $Na_2CO_3$ (w/v %) | Time (min) | Degumming ratio(%) |
|---|---|---|---|
| SF0-30 | 0 | 30 | 25 |
| SF0-60 | 0 | 60 | 28 |
| SF0-90 | 0 | 90 | 30 |
| SF0-120 | 0 | 120 | 31 |
| SF0-150 | 0 | 150 | 33 |
| SF0-180 | 0 | 180 | 33 |
| SF0.5-30 | 0.5 | 30 | 33 |
| SF2.5-30 | 2.5 | 30 | 37 |

The SF aqueous solution was prepared by dissolving 10 g of the dried fibroin fibers in 50 mL of 9 M LiBr solution at room temperature for 24 h. Then the solution was dialyzed against distilled water for 3 days by exchanging dialysis water at every 12 h to remove LiBr salt. The SF aqueous solution concentration was determined by weighing the remaining solid after drying at 100 °C for 1 h. When the high concentration SF aqueous solution was required for electrospinning, the SF aqueous solution was concentrated using PEG solution (50 wt%) as the dialysis solution [20]. The pH values of the SF aqueous solution was adjusted with 5 M NaOH solution for monitoring by pH meter (HI 9811-5N; Hanna Instruments, Chiba, Japan).

### 2.3. Electrospinning of SF aqueous solution

An electrospinning apparatus manufactured by Kato Tech Co. Ltd. (Kyoto, Japan) was used. The SF aqueous solution was placed into a 1 mL syringe (SS-01T; Terumo Corp., Tokyo, Japan) with a 21 gauge stainless needle (NN-2238 N; Terumo Corp., Tokyo, Japan) connected to a high voltage power supply. During electrospinning, applied voltage at 15 kV was applied to SF aqueous solution. The electrospun SF nanofibers were collected on silicon coated paper (Asahikasei home products Co., Ltd., Tokyo, Japan) which was placed at a distance of 18 cm from the needle.

### 2.4. Insolubilizing of SF non-woven mat

As-spun electrospun SF non-woven mat was treated with water vapor and 99.8 vol% methanol to insolubilize it by inducing crystallization of SF [21]. Briefly, for water vapor treatment, the as-spun SF non-woven mat was placed in a desiccator saturated with distilled water vapor by keeping it at 50 °C in an incubator for 10 min. The treated samples were dried at room temperature for 24 h. The desiccator humidity was set to 100RH% for monitoring by a thermal recorder (TR-77U; T and D Corp., Matsumoto, Japan). For methanol treatment, the as-spun SF non-woven mat was immersed in 99.8 vol% methanol for 10 min. Then it was dried for 24 h at room temperature.

### 2.5. Characterization of SF aqueous solution and SF non-woven mat

#### 2.5.1. Viscosity measurement

The SF aqueous solution viscosity was measured at 20 °C using a viscometer (SV-A; A and D Co. Ltd., Tokyo, Japan). Share rate and sample volume were 150 s− 1 and 10 mL respectively. Three samples of each SF aqueous solution were measured, and the results were averaged.

#### 2.5.2. Gel permeation chromatography (GPC)

To measure the molecular weight (Mw) distribution of the SF aqueous

solution, SF aqueous solutions were diluted to 0.1 wt% with an elution buffer (1/15 M pH 7.0 phosphate buffer containing 2 M Urea and 0.1 M Na2SO4). The solutions were filtered through a 0.45 μm hydrophilic PTFE membrane (Merck KGaA, Darmstadt, Germany). A column (8.0 mm × 300 mm, Shodex Protein KW 803; Showa Denko K.K., Tokyo Japan) was used in a high performance liquid chromatograph (HPLC) system (Shimadzu Corp., Kyoto, Japan) equipped with an SPD-M10A UV–Vis detector. The HPLC was operated at a flow rate of 0.5 mL/min at 30 °C. The molecular weight was estimated by calibration using a protein molecular standard (thyroglobulin, apoferritin, β-amylase, aldolase, alcohol dehydrogenase, conalbumin and ovalbumin, Gel Filtration Calibration kit HMW; GE Healthcare Corp., Buckinghamshire, UK).

### 2.5.3. SDS-polyacrylamide gel electrophoresis (SDS-PAGE)

The SF samples in running buffer (Tris-HCl, SDS, sucrose, dithiothreitol (DTT) and bromophenol blue (BPB), E-T520L; ATTO Corp., Tokyo, Japan) were run on a 5–20 wt% polyacrylamide gradient gel (E-T5520L; ATTO Corp., Tokyo, Japan). A molecular marker of 10–245 kDa (WSE-7020; ATTO Corp., Tokyo, Japan) was used for estimation of the SF molecular weight and the distribution. Electrophoresis was performed for 70 min with PageRun-R (ATTO Corp., Tokyo, Japan) using current of 10.5 mA. After electrophoresis, the gel was immersed in a stain solution (EzStain Aqua; ATTO Corp., Tokyo, Japan). Then it was washed with distilled water overnight.

### 2.5.4. Scanning electron microscope (SEM)

The fiber morphologies of as-spun, methanol treated and water vapor treated SF non-woven mats from SF0–120, SF0.5–30 and SF2.5–30 aqueous solutions were observed by scanning electron microscope (SEM: JSM-6010LA; JEOL Ltd., Tokyo Japan) at 10 kV after coating with platinum.

### 2.5.5. Measurement of fiber diameter

The average fiber diameters of SF non-woven mats were measured at 100 different nanofibers of samples from two pictures at random using software (Makijaku Freeware, ver. 1.1.0.0). Histograms of fiber diameter and distribution were drawn using software (OriginPro 8.1; OriginLab Corp., Northampton, USA).

### 2.5.6. Fourier transform infrared spectroscopy (FTIR)

FTIR spectra of the as-spun, water vapor treated and methanol treated SF non-woven mat (2 × 2 cm) were measured using an infrared spectrometer (Prestage-21; Shimadzu Corp., Kyoto, Japan) with ATR equipment (DuraSamplIR; Smith Detection, London, England) in the region of 600–4000 $cm^{-1}$ at room temperature. Spectra were recorded with an accumulation of 30 scans and resolution of 4 $cm^{-1}$.

The amide I (1600–1700 $cm^{-1}$) peaks of the FTIR spectra were decomposed and curve-fitted using software (OriginPro 8.1; OriginLab Corp., Northampton, USA) for analysis of the β-sheet content.

### 2.5.7. Mechanical properties of SF non-woven mat

Mechanical properties of the methanol treated SF non-woven mat (40 × 0.5 mm2) were determined using a test machine (EZ-SX; Shimadzu Corp., Kyoto, Japan) with a 10 N load cell under ambient condition at 20 °C and 65 RH%. The samples with around 300 nm of average fiber diameter were used for tensile test. The sample length was set at 30 mm. The crosshead speed was 10 mm/min. The stress/strain curves were recorded by computer equipped with the test machine and analyzed using software (Trapezium X, version 1.3.1; Shimadzu Corp., Kyoto, Japan). Results were compared by normalization based on the sample weight, attributable to the difficulty to adjust the fiber density in each sample. Five samples of the SF non-woven mat were tested. The results were averaged.

## 3. Results and discussion

### 3.1. Degumming efficiency by boiling water degumming process

Degumming and solubilizing processes are sensitive to fibroin molecular characteristics for electrospinning achievement [22] and [23]. Typical degumming processes reported in the literature were used to boil cocoons in an alkaline solution such as sodium carbonate and sodium bicarbonate aqueous solution with or without a soap such as Marseille soap [24]. This process causes molecular degradation of fibroin attributable to hydrolysis in the alkaline solution [25]. To prevent molecular degradation as much as possible, we degummed the cocoons using boiling water with no alkaline reagents or soaps. Results of degumming by boiling water under various conditions are presented in Table 1. The degumming ratio represents the extent of sericin protein removal; 30% is recognized as successful degumming because the amount of sericin in cocoon fibers is reported as approximately 20–30% of total cocoon weight [26]. Yoon et al. [23] reported that the residual sericin content was 0% at 28.5% of the degumming ratio. Furthermore, Ki et al. described that sericin was removed completely when the degumming ratio was 26.6% [27]. As shown in Table 1, the degumming ratio is much lower than 30% for < 60 min of degumming time. This result suggests that a shorter boiling time is insufficient to remove sericin from cocoon fiber. In contrast, > 150 min of boiling time produces a > 30% degumming ratio. The SF fiber will suffer some damage during longer boiling treatment. The degumming loss by

typical degumming process with sodium carbonate solution is > 30%, which is much higher than that by the boiling water process. Severe conditions such as boiling in alkaline solution cause fibroin degradation and engender weight loss beyond the amount of sericin. This consideration is supported by SEM observation of the degummed fibers. As depicted in Fig. 1, fibers degummed using boiling water treatment for longer than 150 min and by sodium carbonate solution for a shorter time produce many fibrils on the surface comparing with the fiber surface by boiling water treatment for 120 min. These morphology changes indicate SF damage and subsequent degradation of fibroin molecules by hydrolysis. Compared with the fiber morphology before degumming, sericin was apparently removed by the boiling water degumming treatment for 120 min. Sericin could be removed by boiling water degumming, because the degumming ratio of SF0–120 sample was > 30%.

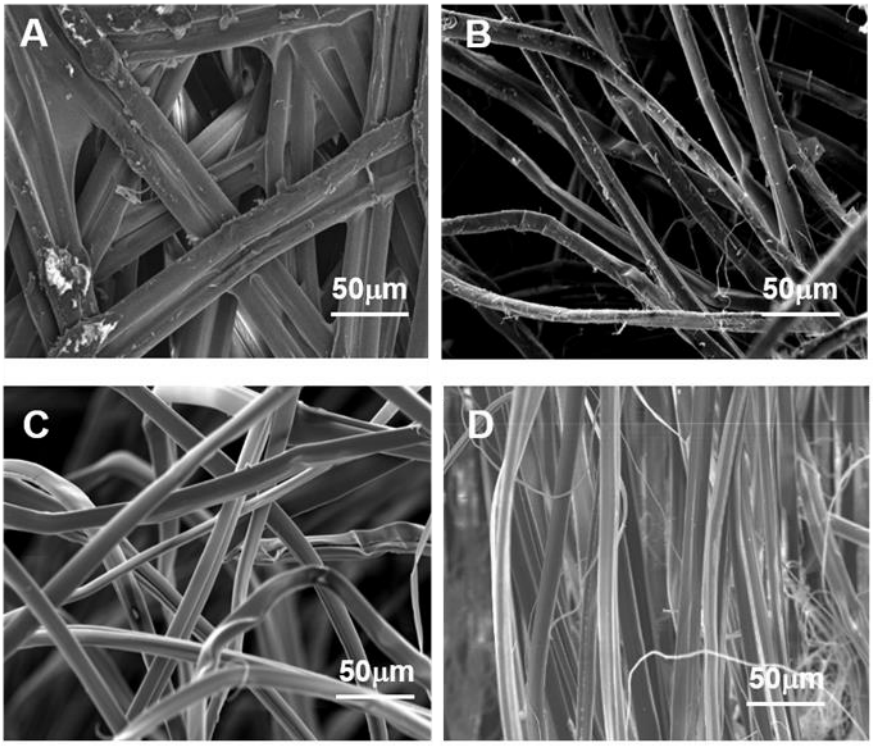


**Fig.1.** SEM photographs of silk fiber before and after different degumming process. (A) before, (B) SF2.5-30, (C) SF0-120, (D) SF0-150. Scale bars present 50mm.

We used an SF0–120 sample for additional analyses and electrospinning studies as a representative sample for boiling water degumming because the sericin removal was achieved with minimal damage to SF fibers.

### 3.2. Molecular degradation by degumming treatment

Fig. 2 presents GPC elution chromatogram and the SDS-PAGE results of the SF aqueous solutions degummed using different process. These results indicate that the fibroin molecules are broken down because of hydrolysis in alkaline solution during degumming. Even by boiling water processes, fibroin degradation occurred: the molecular weight distribution was observed in the GPC elution chromatogram. However, the degree of degradation seems much less than that by alkaline solution degumming. The molecular weight of SF degummed by boiling water process (SF0–120) remained at a much higher value than that by alkaline solution processing (SF0.5–30 and SF2.5–30). The apparent molecular weights at the peak tops of SF0–120, SF0.5–30, and SF2.5–30, were estimated at 203,000, 11,700, and 3100, respectively. SDS-PAGE results clarify the differences of fibroin degradation among the degumming processes. No clear band was observed at lanes 5 and 6 of the samples degummed using a high concentration alkali solution (SF2.5–30). The SF0.5–30 sample lanes presented mostly broad smear staining from 35 kDa to 200 kDa. Slight bands were observed at 324, 311, and 25 kDa. The molecular weight of the fibroin H-chain and L-chain were determined, respectively, at 390 kDa [28] and 25 kDa [29] from gene analyses. These bands might represent the partially degraded H-chains and L-chain. In contrast, SF0–120, the fibroin by the degumming process without alkali, showed a broad band at the higher and narrower molecular range of 180 kDa to 350 kDa than by alkaline processing and clear bands at 25 kDa. This result

indicates that SF degradation might be repressed by treatment without alkali solution for degumming. The boiling water process is effective to keep the molecular weight of SF in the higher range. However, longer treatment time with boiling water caused SF degradation, as shown by the bands at lanes 3 and 4, in which were loaded samples SF0–150 and presented at a lower and wider range of molecular weight than the band of SF0–120.

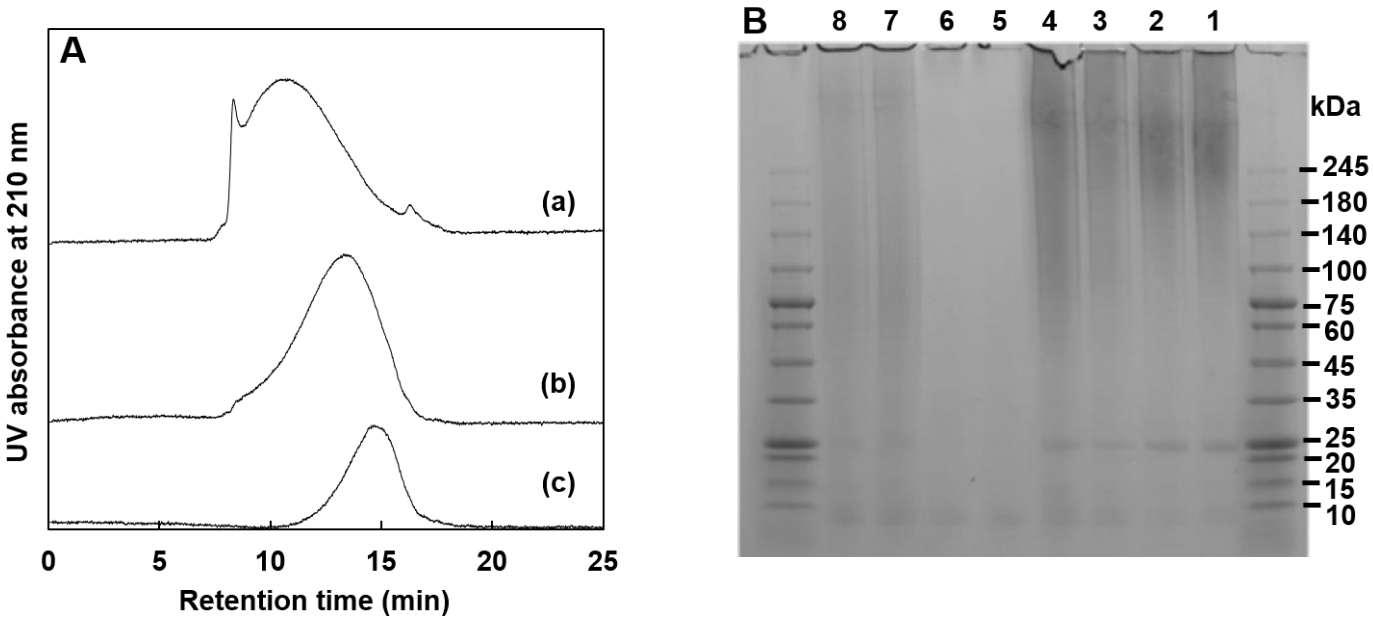


**Fig.2.** Mw and Mw distribution of fibroin in aqueous solution prepared by different degumming process.
A: GPC profiles: (a) SF0-120, (b) SF0.5-30 and (c) SF2.5-30
B: SDS-PAGE, Lane1, 3, 5 and 7 are SF0-120, SF0-150, SF2.5-30 and SF0.5-30 at pH7.0. Lane 2, 4, 6 and 8 are SF0-120, SF0-150, SF2.5-30 and SF0.5-30 at pH10.5

### 3.3. Electrospinning from SF aqueous solution

Several studies to make SF non-woven mat electrospun from SF aqueous solution have been reported. Chen et al. [30] and Wang et al. [31] reported > 28% of SF aqueous solution by 0.5% Na2CO3 degumming process necessary to fabricate the non-woven mat. Cao et al. [20] reported that a low concentration of SF aqueous solution to control the conductivity of the spinning solution with salts such as NaCl and LiBr can form a non-woven mat. However, a > 10% of concentration was required for the fabrication of stable fibers. Jin et al. [17] succeeded in producing a non-woven mat from SF aqueous solution at low concentration with high molecular weight polyethylene oxide (PEO) as a combination spinning solution. However, PEO must be removed from the SF non-woven mat after fabrication. We attempted to produce a SF non-woven mat from our SF aqueous solution degummed by alkaline at up to 22 wt% concentration, but it was difficult to spin the SF fiber using as-prepared SF aqueous solution. Furthermore, even higher molecular weight SF (SF0–120) was incapable of being spun by electrospinning at various concentrations of as-prepared solution.

The electrical charge of spinning solution on electrospinning is important factor to be considered for spinning [32]. Fibroin is protein. Therefore, the net charge of the SF solution is dependent on the pH. We examined the spinning ability of the SF aqueous solution at various pH by electrospinning. Table 2 presents results obtained using SF solutions at various concentrations with each pH. In acidic conditions, no successful fiber was spun from every SF

aqueous solution at up to 22% concentration in this study. Zhu et al. [33] reported that SF aqueous solution adjusted pH at 6.9, which is the same pH as conditions inside the silk glands of silkworms. The solution was able to electro-spin to form the SF non-woven mat. However, a > 30% concentration of SF was necessary for successful electrospinning. The electrospinnability of SF solution in basic conditions was not investigated. The pH dependence of the spinning ability of SF aqueous solution in a basic condition was examined. The results are presented in Table 2. It was difficult to spin from a SF aqueous solution at pH below 10 or at pH above 12. The SF aqueous solutions at pH 10.5, 11, and 11.5 were able to form stable fibers by electrospinning. Especially, a SF aqueous solution at pH 10.5 was spun at 5 wt% concentration in the case of SF0–120. Furthermore, a SF non-woven mat was formed at comparable lower concentrations such as 10% (SF0.5–30) and 16% (SF2.5–30) than reported in literature, even by alkali degumming SF solutions. More than 12 wt% (SF0–120) and 22 wt% (SF0.5–30, SF2.5–30) SF aqueous solution in basic conditions could not be spun in our study because the solution viscosity was too high to flow because of jamming of the fibroin solution into the spinneret nozzle. We infer electrical repulsion among the charged fibroin molecules in basic conditions. We believe that pH 10.5 can serve as adequate repulsion to cause a good fiber jet in an electric field.

**Table 2.** Spinnability of fibroin aqueous solutions at various concentrations and pHs

| Sample code | pH | Concentration of SF aqueous solution (wt%) | | | | | | | | | | | | |
|---|---|---|---|---|---|---|---|---|---|---|---|---|---|---|
| | | 4 | 5 | 6 | 7 | 8 | 9 | 10 | 12 | 14 | 16 | 18 | 20 | 22 |
| SF0-120 | 7 | × | × | × | × | × | × | × | - | - | - | - | - | - |
| | 10.5 | △ | ○ | ○ | ○ | ○ | ○ | ○ | - | - | - | - | - | - |
| | 11 | △ | △ | △ | △ | ○ | ○ | ○ | - | - | - | - | - | - |
| | 11.5 | △ | △ | △ | △ | △ | ○ | ○ | - | - | - | - | - | - |
| SF0.5-30 | 7 | - | - | - | - | × | × | × | × | × | × | × | × | × |
| | 10.5 | - | - | - | - | △ | ○ | ○ | ○ | ○ | ○ | ○ | ○ | ○ |
| SF2.5-30 | 7 | - | - | - | - | × | × | × | × | × | × | × | × | × |
| | 10.5 | - | - | - | - | - | - | - | - | △ | ○ | ○ | ○ | ○ |

○: fibers △: fibers with beads ×: no spinning - : not experiment

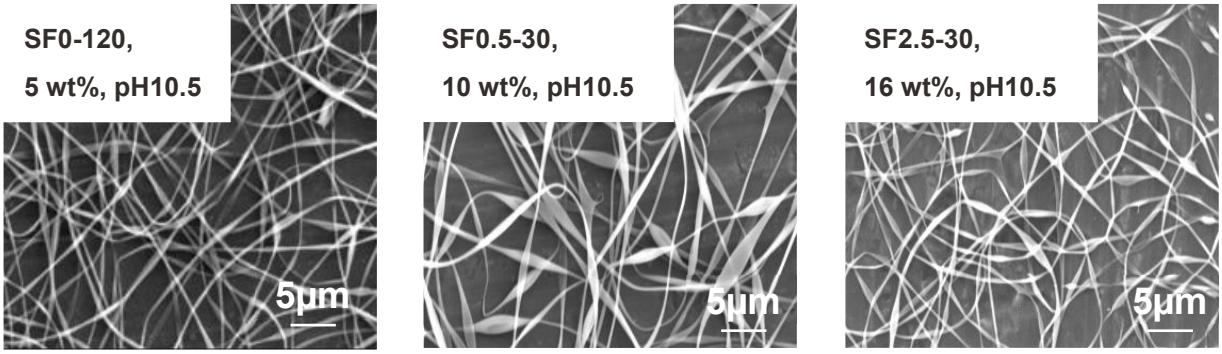

### 3.4. SF aqueous solution viscosity

Viscosity of the polymer solutions used in electrospinning processes is an important factor affecting electrospinnability. Fig. 3 presents the viscosity changes of SF aqueous solutions, SF0–120, SF0.5–30, and SF2.5–30, on the solution concentration. The viscosity increased with the SF concentration. It is particularly interesting that the viscosity ranges of the electrospinnable solution are similar among three samples, although the concentration range of the solution differs. Even though the concentration of SF0–120, SF0.5–30 and SF2.5–30 were different, the lower limit viscosity for electrospinning were similar with > 14 mPa·s. The lower limit concentrations for electrospinning are, respectively, 5, 10, and 16 wt% for SF0–120, SF0.5–30, and SF2.5–30, as shown in Table 2. Therefore, the viscosity range of SF aqueous solutions is estimated from 14 to 100 mPa·s. This result agrees well with the result reported by Cao et al. [20]. The viscosity of the pH 10.5 solution decreased compared with pH unadjusted solution at the same concentration. Electric repulsion among SF molecules in solution at pH 10.5 results in loosening of the molecular entanglement. From the viewpoint of electrospinnability of the SF aqueous solution, the solution viscosity effects are more important than the molecular weight of SF. However, because the solution by the higher molecular weight SF is the higher viscosity at lower concentration than by the lower molecular weight SF, the high molecular weight SF has benefits for electrospinning.

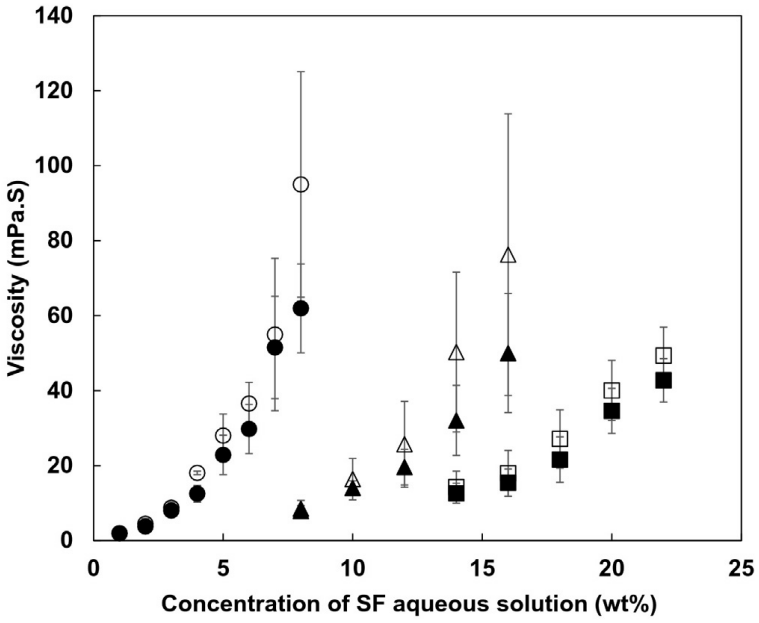


**Fig.3.** Influence of fibroin concentration and pH on viscosity of fibroin aqueous solution.
pH 7 : (○) SF0-120, (△) SF0.5-30, (□) SF2.5-30
pH10.5 : (●) SF0-120, (▲) SF0.5-30, (■) SF2.5-30
Error bars indicate the standard deviations of each data.

### 3.5. Morphology of SF non-woven mat

Fig. 4 portrays the morphology and the diameter distribution of SF no-woven mat from various concentrations of SF aqueous solution at pH 10.5. When the concentrations of SF0–120, SF0.5–30 and SF2.5–30 were 4, 8 and 14 wt% respectively, a bead-like structure in the fiber form exists because the viscosity is too low to maintain a stable jet at the spinneret to break droplets easily in the jet. Stable fiber morphology without beads was observed in the SF non-woven mat from > 5% for SF0–120, 12% for SF0.5–30, and 17% for SF2.5–30. Cylindrical morphology was observed at low concentrations. Ribbon-like morphology was observed at high concentrations. We infer the

following mechanism to form the belt-like structure at high SF concentration [34]. When the fiber is formed during electrospinning, the highly concentrated SF aqueous solution produces the SF thin skin around the fiber quickly. Then water inside the fiber is evaporated gradually. The resulting tube structure is collapsed by atmospheric pressure until the fiber reaches a target and changes the tube to belt-like morphology.

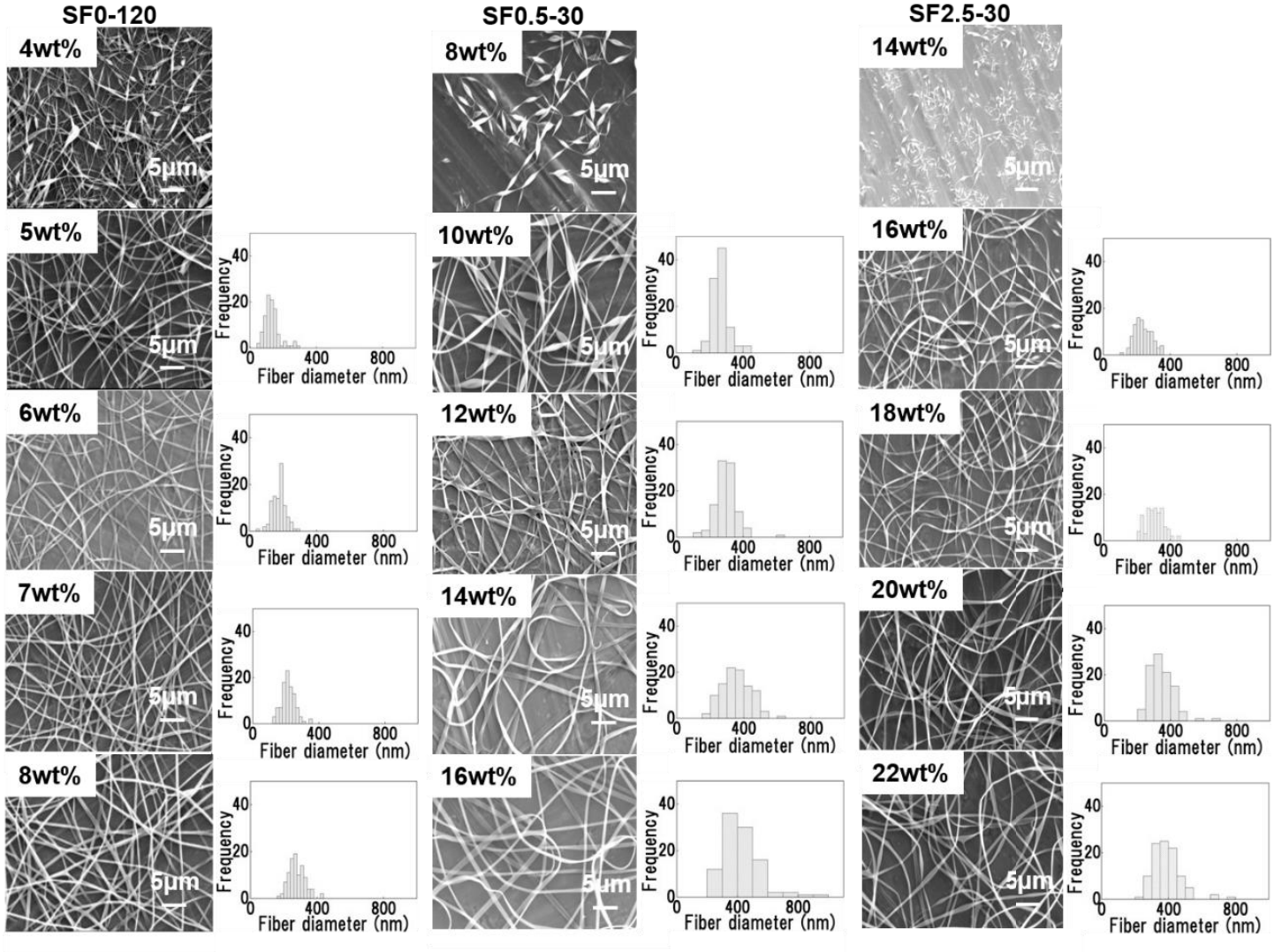


**Fig. 4.** Morphology and fiber diameter distribution of non-woven mat

The fiber diameter distribution did not change much according to the concentration, but a slightly wider distribution was observed at alkaline degumming SF than boiling water degumming SF. The jet of highly concentrated SF aqueous solution at a lower molecular weight might be unstable in an electric field. The average fiber diameter vs. solution concentration is shown in Fig. 5 A. Higher concentrations formed larger diameter fibers [8]. Given the same concentration as shown at 10% and 16% in Fig. 5 A, the fiber diameter spun by a high molecular weight SF is greater than that by a low molecular weight SF. Fig. 5 B presents the relation between solution viscosity and the electrospun fiber diameter. The fiber diameter increased with the solution viscosity. The degumming process also influenced the fiber diameter at the same viscosity of the SF aqueous solution.

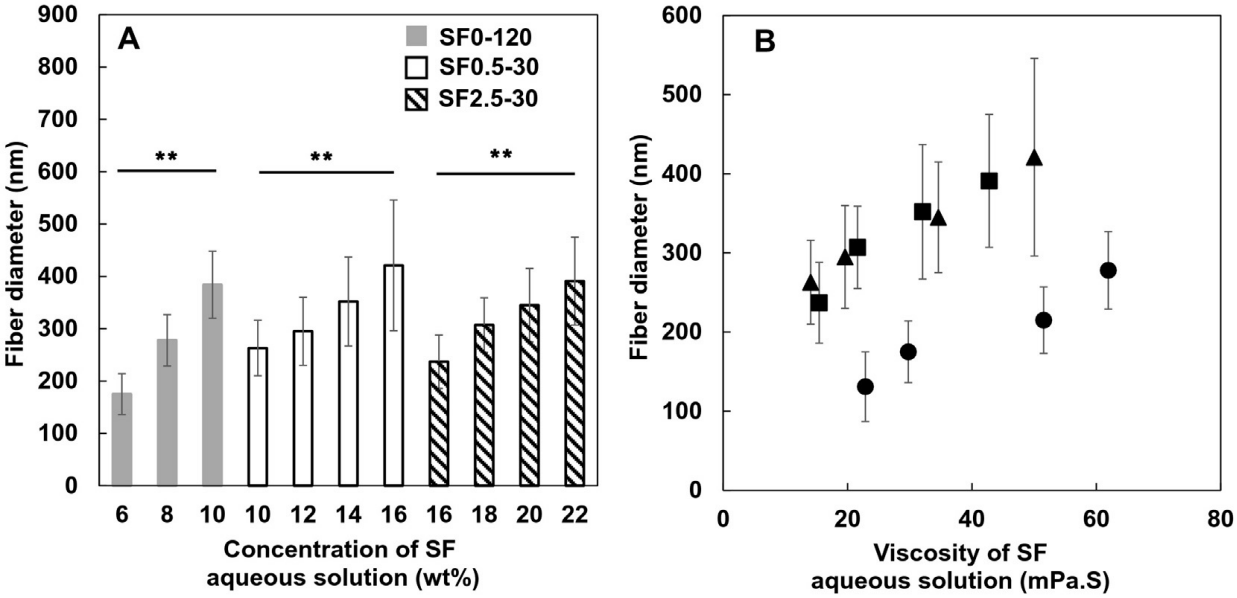


**Fig. 5.** Influence of concentration (A) and viscosity (B) of SF aqueous solution on fiber diameter. (●) SF0-120, (▲) SF0.5-30, (■) SF0.5-30.
Error bars indicate the standard deviations of each data. Statistical significance was determined by Student's t-test and indicated with ** ($p < 0.01$).

### 3.6. Structure of SF non-woven mat before and after insolubilizing treatment

Because the SF non-woven mat as spun mat dissolves easily in water, insolubilizing treatment is necessary to handle the mat. Insolubilizing methods of several kinds have been reported, such as alcohol immersion, alcohol vapor, and water vapor treatment [35], [36] and [37]. We attempted water vapor treatment and methanol treatment to insolubilize our SF non-woven mats. Fig. 6 depicts the morphology and FTIR spectra of the SF non-woven mat from SF0–120, SF0.5–30, and SF2.5–30 before and after insolubilizing treatments. After water vapor treatment, SF0.5–30 and SF2.5–30 fibers were partially swollen, showing fiber shape deformation. In contrast, the fiber shape of SF0–120 was unaffected by water vapor treatment. FTIR spectra show that the secondary structure of all samples transformed by water vapor treatment and methanol treatment and the β-sheet content were increased, which indicates that the SF non-woven mats became water insoluble. Surface characteristics of SF films differ from the bulk characteristics: less β-sheet structure is present near the surface of the SF film than in the bulk part when cast at high temperatures, which implies weak molecular cohesion at the electrospun SF non-woven surface. Therefore, the fiber surfaces of SF0.5–30 and SF2.5–30 are more sensitive to water molecules than SF0–120 is because the molecular weight of SF0.5–30 and SF2.5–30 is lower than SF0–120. Consequently, the fiber shape deformation occurred at SF0.5–30 and SF2.5–30 by water vapor treatment.

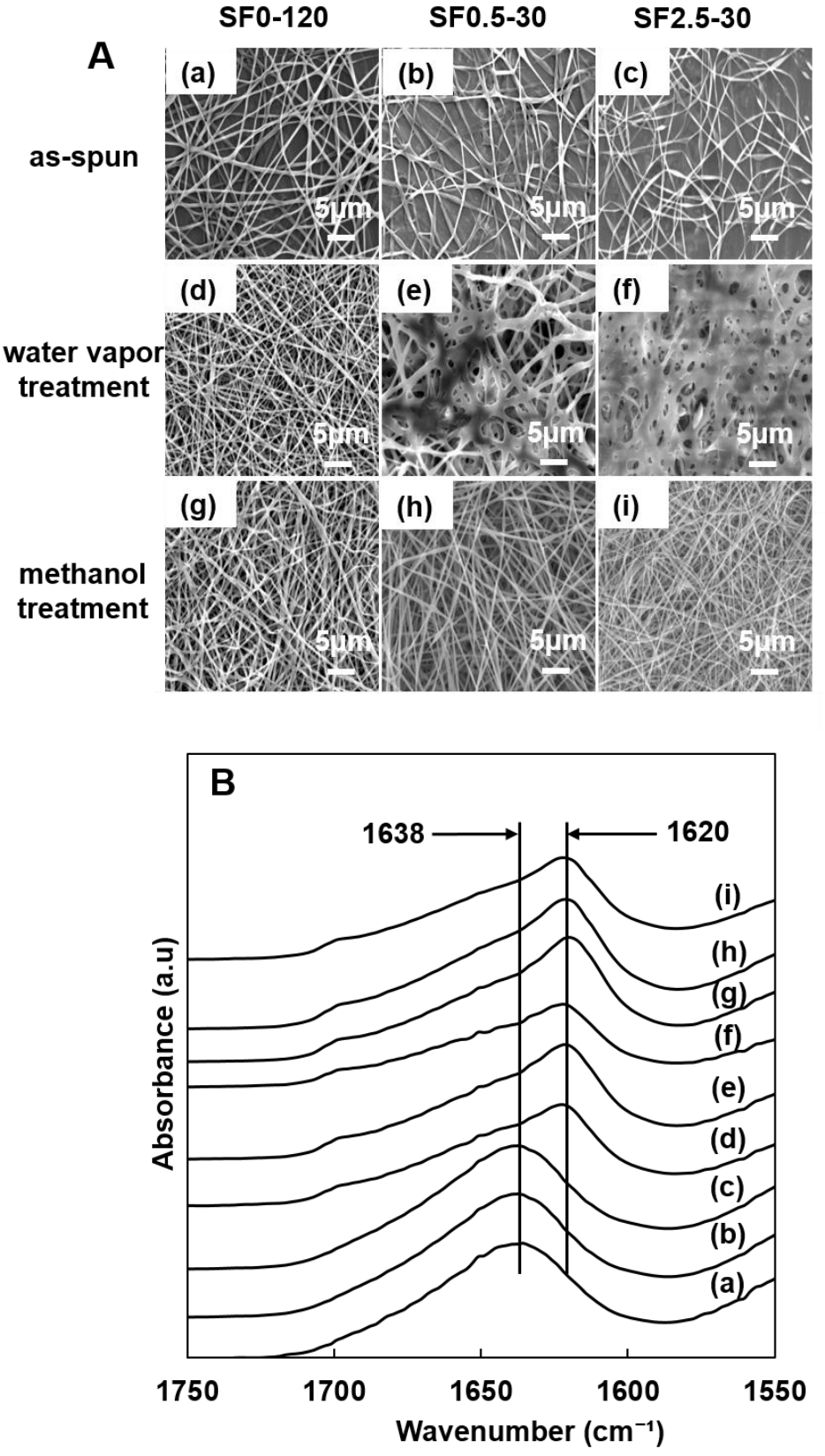
A
SF0-120
SF0.5-30
SF2.5-30
as-spun
water vapor treatment
methanol treatment
(a)
(b)
(c)
(d)
(e)
(f)
(g)
(h)
(i)
5μm
B
1638
1620
(i)
(h)
(g)
(f)
(e)
(d)
(c)
(b)
(a)
Absorbance (a.u)
1750
1700
1650
1600
1550
Wavenumber (cm⁻¹)

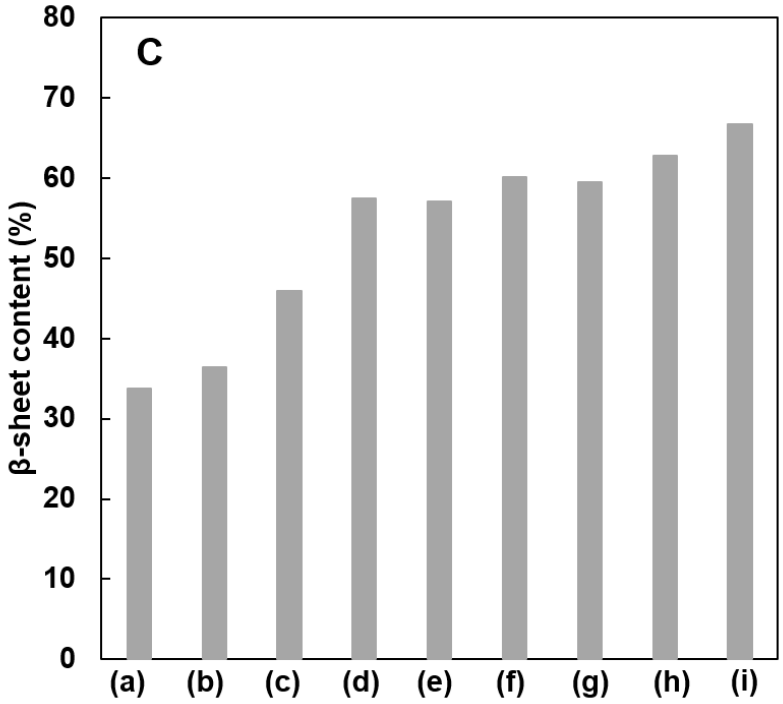


**Fig. 6**. Morphology and FTIR spectra of SF non-woven mat.
A: SEM image: (a–c) as-spun, (d–f) after water vapor treatment and (g–i) methanol treatment.
B: FTIR spectra, C: ß-sheet content: as-spun (a) SF0–120, (b) SF0.5–30, (c) SF2.5–30, after water vapor treatment (d) SF0–120, (e) SF0.5–30, (f) SF2.5–30, and methanol treated (g) SF0–120, (h) SF0.5–30, (i) SF2.5–30.

The morphology and FTIR spectra of the SF non-woven mat after methanol treatment are presented in Fig. 6. As shown in the figure, no morphology change was observed on any sample during treatment. Moreover, the FTIR spectra confirmed that the SF structure changed to ß-sheet rich, indicating that insolubilizing treatment was performed successfully.

### 3.7. Mechanical properties of SF non-woven mat

Fig. 7 presents results of mechanical properties measurements. Typical strain–stress curves of the SF non-woven mat are presented in Fig. 7 A. The SF non-woven mat from SF2.5–30 is weak and brittle, contrary to the SF0–120 non-woven mat which showed high tensile strength and strain resulting in good toughness. Results suggest that the SF molecular weight strongly affected the mechanical behaviors of the SF non-woven mat. The mean tensile stress and strain at breakage of each SF non-woven mat are presented in Fig. 7B and C. The tensile stresses per unit density of non-woven mat (g/m2) are, respectively, 0.83, 0.51, and 0.18 MPa on SF0–120, SF0.5–30, and SF2.5–30. The tensile stress of the SF non-woven mat depends on the molecular weight. A higher molecular weight fiber was able to withstand higher stress. The mean strains at breaking of the SF non-woven mat are, respectively, 11.1, 2.8, and 1.3% on SF0–120, SF0.5–30, and SF2.5–30. The strain of the SF non-woven mat also depends on the SF molecular weight. However, the molecular weight dependence on mechanical properties of the SF non-woven mat must be discussed carefully because the mechanical properties of the SF non-woven mat are determined not only by the properties of the respective fibers but also by the distributions of fiber diameter, the orientations of fibers, and the fiber density of the SF non-woven mats. This study evaluated the strain per unit density of a non-woven mat, which revealed that the distribution of fiber diameter and orientation of fibers are similar among samples, as shown in Fig. 2. Therefore, we conclude that the molecular weight of SF influences the

mechanical properties of the electrospun SF non-woven mat. Quantitative discussions of tensile test results for a SF non-woven mat and comparison with other studies are difficult for the reason presented above. Several reports have described tensile studies of SF non-woven mats produced from a SF aqueous solution. The apparent stress and strain at the break point of a SF non-woven mat was reported, respectively, as 11.7 ± 0.7 MPa and 10.2 ± 1.6% by Cao et al. [20] and 1.49 MPa and 1.63% by Chen et al. [30]. In our study, 0.8 ± 0.1 MPa and 12 ± 5.6% of the apparent tensile stress and strain were found for an SF0–120 non-woven mat. Our results could not be compared simply with the other reported results because the fiber density in the cross-sectional area is not equal among the samples used in each study. Nevertheless, it can be said that the SF0.5–30 non-woven mat was formed using almost identical processes to those reported by Cao et al. [20]. The tensile stress and strain at the break point of SF0.5–30 were, respectively, 0.51 ± 0.05 MPa and 2.4 ± 0.4%. Therefore, the SF0–120 non-woven mat described in this report represents 1.6 times the strength and four times the elongation of an SF0.5–30 non-woven mat formed by SF from the typical degumming process. This result indicates that a SF non-woven mat from high molecular weight SF aqueous solution fabricated in this study shows good mechanical properties.

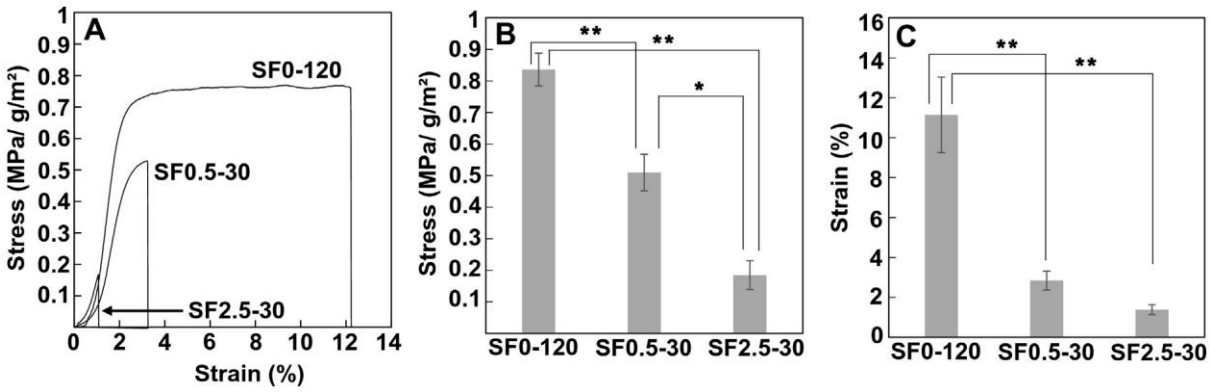


**Fig. 7.** Mechanical properties of SF non-woven mat by different SF aqueous solution.

A: Typical stress-strain curve of SF non-woven mat.

C: Influence of degumming conditions on strain of SF non-woven mat (*, $p < 0.01$ by t-test).

Error bars indicate the standard deviations of each data. Statistical significance was determined by Student's t-test and indicated with * ($p < 0.05$) and **($p < 0.01$).

## 4. References

[1] H. Tao, D.L. Kaplan, F.G. Omenetto, Silk materials—a road to sustainable high technology, Adv. Mater., 24 (21) (2012), pp. 2824–2837.

[2] S. Kujala, A. Mannila, L. Karvonen, K. Kieu, Z. Sun, Natural silk as a photonics component: a study on its light guiding and nonlinear optical properties, Sci. Rep., 6 (2016), p. 22358.

[3]C. Vepari, D.L. Kaplan, Silk as a biomaterial, Prog. Polym. Sci., 32 (8–9) (2007), pp. 991–1007.

[4] B. Kundu, N.E. Kurland, S. Bano, C. Patra, F.B. Engel, V.K. Yadavalli, S.C. Kundu, Silk proteins for biomedical applications: bioengineering perspectives Prog. Polym. Sci., 39 (2) (2014), pp. 251–267.

[5] C. Krishna, S. Pillai, C.P. Sharma, Absorbable polymeric surgical sutures, chemistry, production, properties, biodegradability, and performance, J. Biomater. Appl., 25 (2010), pp. 291–366.

[6] D.N. Rockwood, R.C. Preda, T. Yucel, X. Wang, M.L. Lovett, D.L. Kaplan, Materials fabrication from Bombyx mori silk fibroin, Nat. Protoc., 6 (10) (2011), pp. 1612–1631.

[7] T.G. Kim, H. Shin, D.W. Lim, Biomimetic scaffolds for tissue engineering, Adv. Funct. Mater, 22 (12) (2012), pp. 2446–2468.

[8] S. Sukigara, M. Gandhi, J. Ayutsede, M. Micklus, F. Ko, Regeneration of Bombyx mori silk by electrospinning—part 1_processing parameters and geometric properties, Polymer, 44 (2003), pp. 5721–5727.

[9] F. Zhang, B. Zou, Z. Fan, Z. Xie, Q. Lu, X. Zhang, D.L. Kaplan, Mechanisms and control of silk-based electrospinning, Biomacromolecules, 13 (3) (2012), pp. 798–804.

[10] K. Ohgo, C. Zhao, M. Kobayashi, T. Asakura, Preparation of non-woven nanofibers of Bombyx mori silk, Samia cynthia ricini silk and recombinant hybrid silk with electrospinning method, Polymer, 44 (3) (2003), pp. 841–846.

[11] S. Zarkoob, R.K. Eby, D.H. Reneker, S.D. Hudson, D. Ertley, W.W. Adams Structure and morphology of electrospun silk nanofibers, Polymer, 45 (11) (2004), pp. 3973–3977.

[12] A.J. Meinel, K.E. Kubow, E. Klotzsch, M. Garcia-Fuentes, M.L. Smith, V. Vogel, H.P. Merkle, L. Meinel, Optimization strategies for electrospun silk fibroin tissue engineering scaffolds, Biomaterials, 30 (2009), pp. 3058–3067.

[13] X. Zhang, M.R. Reagan, D.L. Kaplan, Electrospun silk biomaterial scaffolds for regenerative medicine, Adv. Drug Deliv. Rev., 61 (12) (2009), pp. 988–1006.

[14] G.H. Altman, F. Diaz, C. Jakuba, T. Calabro, R.L. Horan, J. Chen, H. Lu, J. Richmond, L.D. Kaplan, Silk-based biomaterials, Biomaterials, 24 (2003), pp. 401–416.

[15] H. Wang, Y. Zhang, H. Shao, X. Hu, Electrospun ultra-fine silk fibroin fibers from aqueous solutions, J. Mater. Sci., 40 (20) (2005), pp. 5359–5363.

[16] A. Matsumoto, J. Chen, A.L. Collette, U.J. Kim, G.H. Altman, P. Cebe, D.L. Kaplan, Mechanism of silk fibroin sol-gel transitions, J. Phys. Chem. B, 110 (2006), pp. 21630–21638.

[17] H.-J. Jin, S.V. Fridrik, G.C. Rutledge, D.L. Kaplan, Electrospinning Bombyx mori silk with poly(ethylene oxide), Biomacromolecules, 3 (2002), pp. 1233–1239.

[18] M. Wang, H.-J. Jin, D.L. Kaplan, G.C. Rutledge, Mechanical properties of electrospun silk fibers, Macromolecules, 37 (2004), pp. 6856–6864.

[19] H.J. Jin, J. Chen, V. Karageorgiou, G.H. Altman, D.L. Kaplan, Human bone marrow stromal cell responses on electrospun silk fibroin mats,

Biomaterials, 25 (2004), pp. 1039–1047.

[20] H. Cao, X. Chen, L. Huang, Z. Shao, Electrospinning of reconstituted silk fiber from aqueous silk fibroin solution, Mater. Sci. Eng. C, 29 (7) (2009), pp. 2270–2274.

[21] B.-M. Min, L. Jeong, K.Y. Lee, W.H. Park, Regenerated silk fibroin nanofibers: water vapor-induced structural changes and their effects on the behavior of normal human cells, Macromol. Biosci., 6 (4) (2006), pp. 285–292.

[22] J.S. Ko, K. Yoon, C.S. Ki, H.J. Kim, D.G. Bae, K.H. Lee, Y.H. Park, I.C. Um, Effect of degumming condition on the solution properties and electrospinnablity of regenerated silk solution, Int. J. Biol. Macromol., 55 (2013), pp. 161–168.

[23] K. Yoon, H.N. Lee, C.S. Ki, D. Fang, B.S. Hsiao, B. Chu, I.C. Um, Effects of degumming conditions on electro-spinning rate of regenerated silk, Int. J. Biol. Macromol., 61 (2013), pp. 50–57.

[24] F. Wang, T.-T. Cao, Y.-Q. Zhang, Effect of silk protein surfactant on silk degumming and its properties, Mater. Sci. Eng. C Mater. Biol. Appl., 55 (2015), pp. 131–136.

[25] H. Dou, B. Zuo, Effect of sodium carbonate concentrations on the degumming and regeneration process of silk fibroin, J. Text. Inst., 106 (3) (2015), pp. 311–319.

[26] M. Mondal, K. Trivedy, S.N. Kumar, The silk proteins, sericin and fibroin in silkworm, Bombyx mori Linn., - a review, Caspian J. Env. Sci., 5 (2) (2007), pp. 63–76.

[27] C.S. Ki, J.W. Kim, H.J. Oh, K.H. Lee, Y.H. Park, The effect of residual silk sericin on the structure and mechanical property of regenerated silk filament, Int. J. Biol. Macromol., 41 (3) (2007), pp. 346–353.

[28] C.-Z. Zhou, F. Confalonieri, N. Medine, Y. Zivanovix, C. Esnault, T. Yang,

M. Jacquet, J. Janin, M. Duguset, R. Perasso, Z.-G. Li, Fine organization of Bombyx mori fibroin heavy chain gene, Nucleic Acids Res., 28 (12) (2000), pp. 2143–2419.

[29] K. Yamaguchi, Y. Kikuchi, T. Takagi, A. Kikuchi, F. Oyama, K. Shimura, S. Mizuno, Primary structure of the silk fibroin light chain determined by cDNA sequencing and peptide analysis, J. Mol. Biol., 210 (1980), pp. 127–139.

[30] C. Chen, C. Chuanbao, M. Xilan, T. Yin, Z. Hesun, Preparation of non-woven mats from all-aqueous silk fibroin solution with electrospinning method, Polymer, 47 (18) (2006), pp. 6322–6327.

[31] H. Wang, H. Shao, X. Hu, Structure of silk fibroin fibers made by an electrospinning process from a silk fibroin aqueous solution, J. Appl. Polym. Sci., 101 (2) (2006), pp. 961–968.

[32] T.J. Sill, H.A. von Recum, Electrospinning: applications in drug delivery and tissue engineering, Biomaterials, 29 (13) (2008), pp. 1989–2006.

[33] J. Zhu, H. Shao, X. Hu, Morphology and structure of electrospun mats from regenerated silk fibroin aqueous solutions with adjusting pH, Int. J. Biol. Macromol., 41 (4) (2007), pp. 469–474.

[34] S. Koombhongse, W. Liu, D.H. Reneker, Flat polymer ribbons and other shapes by electrospinning, J. Polym. Sci. B Polym. Phys., 39 (2001), pp. 2598–2606.

[35] H.-J. Jin, J. Park, V. Karageorgiou, U.-J. Kim, R. Valluzzi, P. Cebe, D.L. Kaplan, Water-stable silk films with reduced ß-sheet content, Adv. Funct. Mater., 15 (8) (2005), pp. 1241–1247.

[36] X. Hu, D.L. Kaplan, P. Cebe, Determining beta-sheet crystallinity in fibrous proteins by thermal analysis and infrared spectroscopy, Macromolecules, 39 (2006), pp. 6161–6170.

[37] X. Hu, K. Shmelev, L. Sun, E.-S. Gil, S.-H. Park, P. Cebe, D.L. Kaplan

Regulation of silk material structure by temperature-controlled water vapor annealing, Biomacromolecules, 12 (5) (2011), pp. 1686–1696.

# Chapter 4: Production of three-dimensional silk fibroin nanofiber non-woven fabric by wet electrospinning

## Chapter 4: Production of three-dimensional silk fibroin nanofiber non-woven fabric by wet electrospinning


### Abstract

Three-dimensional (3D) silk fibroin (SF) nanofiber non-woven fabric was fabricated by wet electrospinning (WES) using SF aqueous spinning solution and a liquid bath as a collector. Citric acid buffered solution at pH 3.8 supplemented with t-butyl alcohol (t-BuOH) was used as the liquid bath. The t-BuOH concentration influenced the apparent pore size and porosity of the WES non-woven fabric. The maximum pore size was formed at 30% of t-BuOH. The as-spun WES non-woven fabric structure had a crystallized form. Cell adhesion on the WES non-woven fabric was lower than that produced on the non-woven fabric by traditional dry electrospinning (DES), but no difference was observed in cell proliferation rates between WES and DES non-woven fabrics. Cells adhered and proliferated on both the surface and the inner spaces of WES non-woven fabric, although cells adhered only on the surface of DES non-woven fabric consisting of high fiber density. The WES non-woven fabric is anticipated for use as a cell scaffold mimicking an extracellular matrix in tissue.

## 1. Introduction

Regenerated silk fibroin (SF) materials such as films, sponges, and electrospun non-woven fabric have been studied for use as cell scaffolds because of their biocompatibility and good mechanical properties [1,2]. Recently, many studies have examined electrospun SF non-woven fabrics, investigating the preparation of silk fibroin solution [3–5] conformational and mechanical properties [6,7] and cell cytotoxicity [2] because the nanofiber network in the non-woven fabric can simulate tissue extracellular matrix (ECM) construction [8]. Three-dimensional construction with porous structure mimicking a tissue ECM produces a cell scaffold that facilitates tissue regeneration [9]. However, nanofibers electrospun using dry electrospinning (DES) deposition on a flat plate or rotating drum accumulated into a mass at high fiber densities. No construction of nanofiber networks with high porosity, such as an ECM framework, is done using a conventional method such as DES.

To resolve that difficulty, modified electrospinning has been reported, such as using a micro-patterned template like a honeycomb structure [10], applying a deionizer for eliminating the electricity of electrospun mat [11], using co-spun microparticles to be removed after spinning [12], and using bubbles generated chemically [13]. Nevertheless, these techniques are extremely complicated. No method of simple application to an SF system has been reported in the relevant literature.

Wet electrospinning, which combines electrospinning and wet spinning can be used to fabricate three-dimensional (3D) non-woven fabric with high

porosity. Actually, wet electrospinning consists of conventional electrospinning with a liquid bath as the collector [14]. Ki et al. [15, 16] reported 3D SF nanofiber fabrics produced using wet electrospinning. The spinning solution was an SF formic acid solution. Methanol was used as the liquid bath collector. Formic acid and methanol are harmful to living organisms and are hazardous during fabrication processes. These reagents are therefore best avoided when producing medical materials such as cell scaffolds.

For this study, 3D SF nanofiber non-woven fabrics with high porosity were produced using wet electrospinning with SF aqueous spinning solution and water-based liquid bath as the collector. The 3D non-woven fabric was characterized by pore size, secondary structure, cell adhesion, and proliferation compared with the non-woven fabric produced using DES.

## 2. Materials and methods

### 2.1 Materials

*Bombyx mori* silkworm cocoons were provided generously by the experimental farm at Shinshu University. Chemical reagents, lithium bromide (LiBr), methanol, t-butanol (t-BuOH), citric acid, sodium citrate, and sodium hydroxide (NaOH), purchased from Wako Pure Chemical Industries Ltd. (Tokyo, Japan), were used without further purification. Cellulose dialysis membranes (molecular weight cut-off: 12,000–14,000 Da) were purchased from Kenis Ltd. (Tokyo, Japan).

### 2.2 Preparation of SF spinning solution

Silk cocoons suspended in boiling water at a 1:200 bath ratio and were kept at 95–98°C for 2 h to remove sericin. To prevent molecular degradation during degumming process to the greatest degree possible in this study, we used boiling water as the degumming solution, without alkaline reagents such as sodium carbonate [17]. Then the degummed fibers were washed thoroughly in water for 1 h and were dried overnight at room temperature. After the dried silk fibroin (SF) fibers were weighed, the degumming ratio was calculated using the following equation.

$$degumming\ ratio = \frac{W_1 - W_2}{W_1} \times 100$$

Therein, W1 and W2 respectively denote the cocoon weight and degummed fiber weight. The degumming ratio was confirmed as more than 30%.

The degummed SF fibers were dissolved in 9 M LiBr for 24 h at room temperature. Then the solutions were dialyzed against distilled water for 3 days in a cellulose dialysis membrane. The dialysate was changed every 12 h. Using a pH meter, the SF aqueous spinning solution pH was adjusted to 10.5 using 5M NaOH solution [18].

### 2.3 Wet electrospinning and Dry Electrospinning

A modified electrospinning apparatus manufactured by MECC Co. Ltd. (Fukuoka, Japan) was used for wet electrospinning (WES) experiments. A stainless steel tray (150 × 200 × 20 mm) liquid bath filled with 0.05 M citric acid buffer mixed with ethanol and tert-butyl alcohol (t-BuOH) was placed on the electrode plate as the collector. The SF aqueous spinning solution at 6 wt% was put into a 5 mL disposable syringe (SS-05SZ; Terumo Corp., Tokyo, Japan) with a 21-gauge stainless needle (NN-2238 N; Terumo Corp., Tokyo, Japan) connected to a high-voltage power supply. Wet electrospinning was done at room temperature for 1 h under the following conditions, with applied voltage and distance between the needle and the liquid bath of 15 kV and 18 cm, respectively. The spinning rate was 1.0 ml/h. Before evaluation, the wet electrospun SF non-woven fabrics were freeze-dried using a freeze-dryer (FD-5N; Tokyo Rikakikai Co. Ltd., Tokyo, Japan).

An electrospinning apparatus (Kato Tech Co. Ltd. Kyoto, Japan) with a

plane surface collector was used for traditional DES. The dry electrospun SF nanofibers were collected on silicon-coated paper (Asahikasei Home Products Co.,Ltd., Tokyo, Japan) placed 18 cm distant from the needle. The DES was performed using SF aqueous spinning solution under the same conditions as those used for WES. The respective thicknesses of WES and DES non-woven fabrics spun at this condition were approximately 50 and 20 μm.

### 2.4 Characterization of WES and DES non-woven fabric

The WES and DES non-woven fabric morphologies were observed using a scanning electron microscope (SEM: JSM-6010LA; JEOL Ltd., Tokyo Japan) at 10 kV after coating with platinum. For each SEM image, the average pore sizes and average fiber diameters of WES and DES non-woven fabrics were measured at 100 different points using software (Makijaku Freeware, ver. 1.1.0.0).

FTIR spectra of the non-woven fabrics were obtained using an infrared spectrometer (Prestage-21; Shimadzu Corp., Kyoto, Japan) with ATR equipment (DuraSamplIR; Smiths Detection, London, England) in the region of 600–4000 $cm^{-1}$ at room temperature. The spectra were recorded at resolution of 4 cm-1 and 30 scan accumulation.

Peak separation and curve fitting of the FTIR spectra at the amide I region was performed by Origin 8.1 (OriginLab Corp., Northampton, USA). The baseline was set linearly between two points of 1600 $cm^{-1}$ and 1700 $cm^{-1}$. The second derivative was applied to the original spectra in the amide I region without smoothing treatment to set the peak tops for peak separations and

the Gaussian function was used for curve fitting of each peak. The ß-sheet content was determined by integrating the area of each peak attributed to ß-sheet structure according to an earlier report [19].

### 2.5 Cell culture test

For cell culture tests, the dried DES and WES non-woven fabrics were sterilized using dry heat sterilization at 180°C for 30 min. NIH3T3 cells were provided by the Riken BRC cell bank (Tsukuba, Japan). After 12 mm disks of sterilized WES and DES non-woven fabric were punched out of the respective materials, they were put in 48 multi-well dishes (Nunc; Thermo Fisher Scientific K.K., Kanagawa, Japan). Eagle MEM (Nissui Pharmaceutical Co. Ltd., Tokyo, Japan) with 10% fetal bovine serum (Gibco, Invitrogen Co., USA) and 0.01 wt% of kanamycin antibiotic was used for the culture medium. The cell suspension was put into WES and DES non-woven fabric at 5000 cells/sample. Cells were cultured under 37°C and 5% CO2. Cell numbers in WES and DES non-woven fabric were inferred from lactate dehydrogenase (LDH) consumption. At 1, 3, 5, and 7 days of culture, each sample was put into 0.5% Triton X-100/PBS solution to dissolve the cells in the WES and DES non-woven fabric. Then the LDH activity of the dissolved solution was measured using the kinetics of NADH-consuming reactions at 340 nm absorbance. The cell number was calculated using LDH activity with calibration. Three samples were measured at each culture day. Then the data were averaged. Statistical analyses were conducted using Student t-tests, for

which $p<0.05$ was inferred as significant.

## 3. Results and discussion

### 3.1 Wet electrospinning

For the liquid bath in the wet electrospinning system (WES), a water-based solution is preferred for simulation of a living body in medical use and during the production process. However, water was inapplicable for the solution because the electrospun SF nanofibers dissolved quickly in water and were unable to produce a non-woven fabric with 3D form. Because the isoelectronic point of silk fibroin is reported at pH 4.0 [20], the pH of the solution in the liquid bath was adjusted to around pH 4 using buffer solutions to cause SF fiber coagulation. The citric acid buffer solution at pH 3, 3.8, and 5 worked efficiently to form the non-woven fabric on the liquid bath. However, no 3D fabric was observed. Moreover, the fabric morphology resembled that of non-woven fabrics (2D) formed by conventional dry electrospinning (DES). The electrospun SF fibers accumulated only on the solution surface in the liquid bath, as on the dry solid electrode in the DES system. The high surface tension of citric acid aqueous buffer obstructed immersion of the electrospun SF fibers into the liquid bath solution. Yokoyama et al [14] reported that when the water (surface tension: 72 mN/m) was used as a liquid bath, wet electrospun poly (glycolic acid) (PGA) nanofibers floated on the water because of its high surface tension. We added alcohols in an attempt to reduce the surface tension of the citric acid aqueous buffer. Figure 1 presents morphologies of the WES non-woven fabrics formed in the citric acid buffer

with ethanol (22.31 mN/m surface tension, [21]) and tert-butyl alcohol (t-BuOH, surface tension: 18.16 mN/m, [14]). Both alcohols were effective to immerse the SF nanofibers into the liquid bath and spin to the 3D fabric form with expanding gaps among fibers, but higher ethanol concentration was necessary to form the 3D non-woven fabric than that used for t-BuOH, as presented in Fig. 1. Therefore, for the WES system, we selected t-BuOH added to the citric acid buffer as the liquid bath solution.

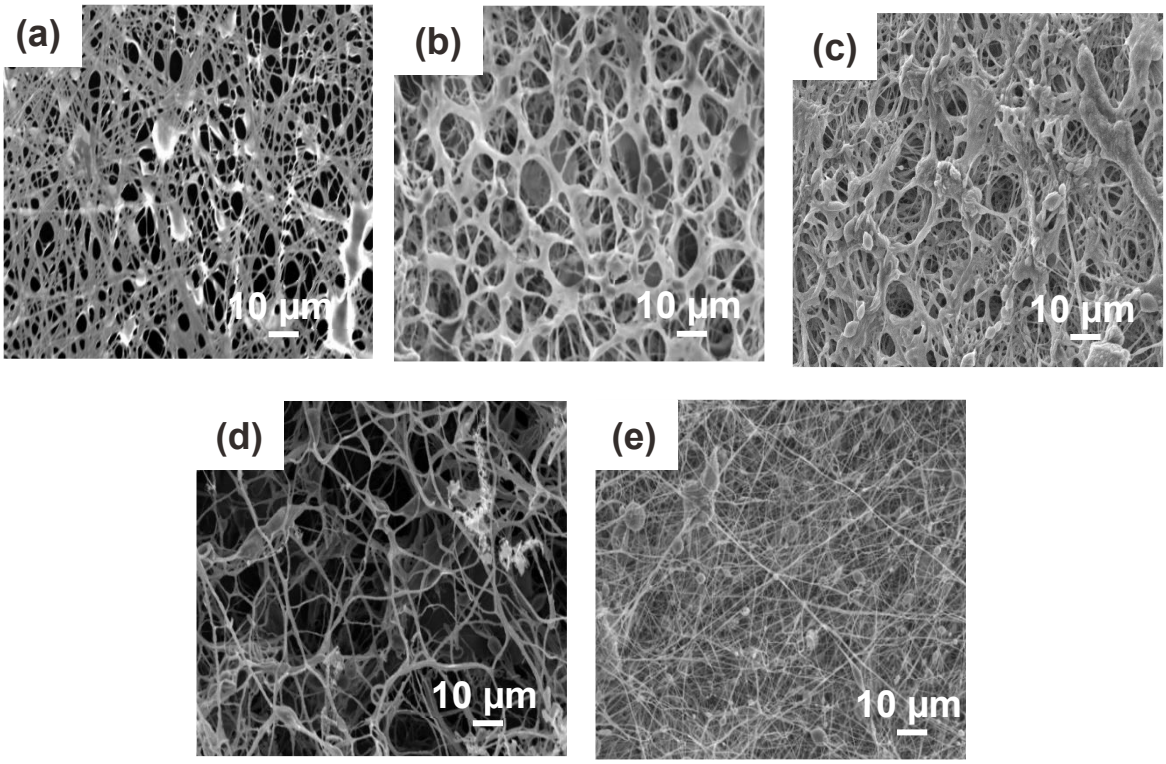


**Fig.1.** SEM images of WES non-woven fabrics formed in citric acid buffer at pH 3.8 with (a) 0 vol%, (b) 50 vol%, (c) 70 vol% of ethanol and with (d) 30 vol%, (e) 70 vol% of t-BuOH.

### 3.2 Influence of t-BuOH concentration on WES non-woven fabric morphology

Figure 2 presents SEM images of WES non-woven fabric formed using the liquid bath containing 10–50 vol% t-BuOH. The t-BuOH concentration influenced the morphology, fiber density, and porosity of the WES non-woven fabric. Results show that no clear nanofiber morphology was formed using the t-BuOH solution at 10% or 20% concentration. The reduction of the surface tension by addition of t-BuOH at less than 20% was insufficient to immerse the electrospun SF nanofibers into the solution. Therefore, the nanofibers were unable to disperse in the solution. Instead, they accumulated on the solution surface. A nanofiber network in the non-woven fabric was fabricated at more than 30% of the t-BuOH solution. The fiber density increased and the porosity decreased according with the increase of the t-BuOH concentration from 30% to 50 vol%. These phenomena are explained by the fact that the amount of soaked electrospun SF nanofibers in the liquid bath increased along with the t-BuOH concentration because of the lower surface tension of the solution. Great amounts of the soaked SF nanofibers can become mutually entangled at higher concentrations of t-BuOH, resulting in denser fiber density and lower porosity in the WES non-woven fabric. Figure 3 presents the apparent average pore size of the WES non-woven fabric estimated from SEM images against the t-BuOH concentration. Around 12 μm of average pore size was formed in the 3D SF non-woven fabric by WES using a 30% t-BuOH solution. The average pore size can be controlled by changing the t-BuOH concentration in the liquid bath. The respective average fiber

diameters of WES and DES non-woven fabrics were approximately 450 nm and 180 nm. The t-BuOH concentration in the liquid bath did not affect the average fiber diameter. We infer that the difference between WES and DES fibers causes shrinkage of the fibers with DES during drying on the collector while the fibers in the liquid bath retained the as-spun fiber diameter because of coagulation in the liquid bath at the time of collection. This result shows good agreement with results reported elsewhere in the literature [15].

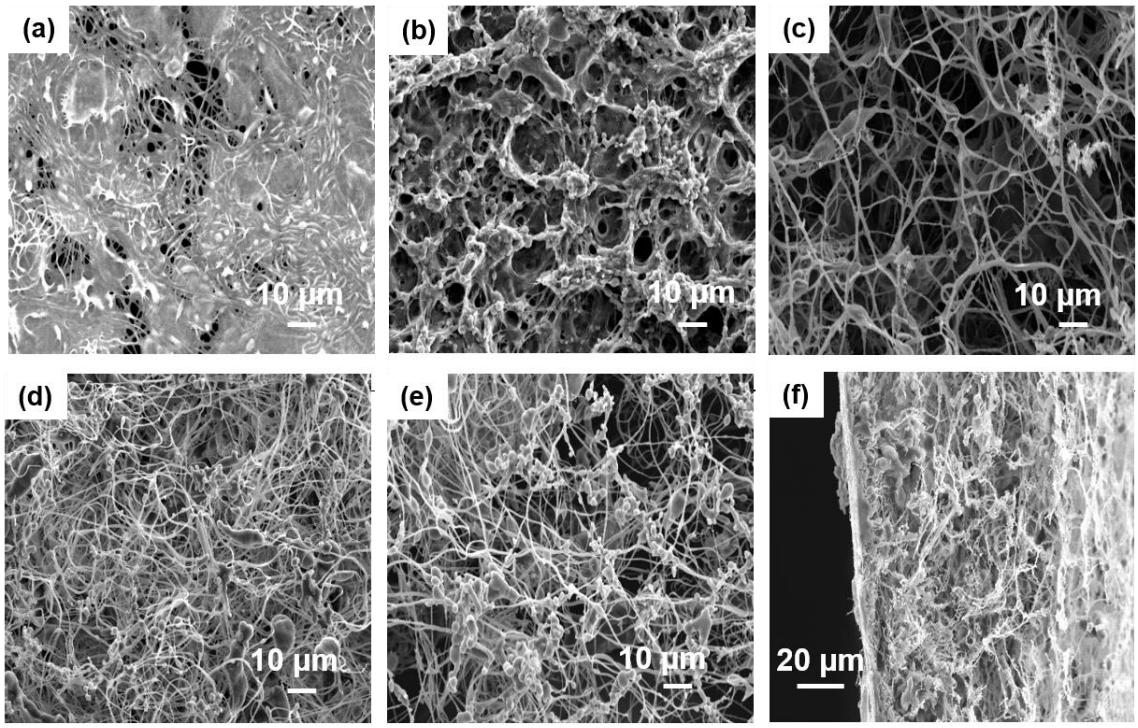


**Fig. 2.** SEM images of WES non-woven fabrics formed in citric acid buffer at pH 3.8 with (a) 10 vol%, (b) 20 vol%, (c) 30 vol%, (d) 40 vol% and (e) 50 vol% of t-BuOH and (f) cross sectional SEM image of WES non-woven fabric formed in citric acid buffer at pH 3.8 with 30 vol% of t-BuOH.

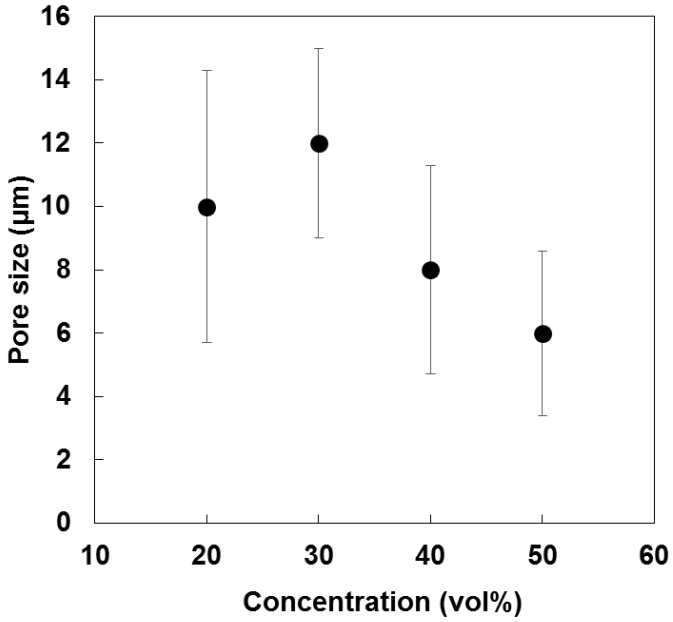


**Fig.3.** Influence of t-BuOH concentration on pore size of WES non-woven fabrics (n=100). Error bars indicate the standard deviations.

### 3.3 Secondary structure of SF nanofibers in WES non-woven fabric

FTIR spectroscopy was applied to ascertain the electrospun SF nanofiber structure in the fabrics. Figure 4A portrays the amide I region of the spectra, which presents the secondary structure of the as-spun and methanol treated DES non-woven fabric, as-spun WES non-woven fabric using only citric acid buffer, and the as-spun WES non-woven fabric using citric acid buffer with 30 vol% and 50 vol% of t-BuOH. An adsorption peak at 1622 $cm^{-1}$, which is attributed to the ß-sheet structure [18] and the crystallized form of SF, appeared on the as-spun WES non-woven fabric. These results indicate the WES non-woven fabric was crystallized at the same time as collection in the liquid bath by coagulation of SF at isoelectronic pH. The as-spun DES non-woven fabric had a non-crystallized structure, as indicated by the adsorption peak at 1641 $cm^{-1}$, which is attributed to its random coil structure [22] and non-crystallized form of SF. These results suggest that non-crystallized SF nanofibers were spun during electrospinning, and that the SF nanofiber structure was transformed to a crystallized form in the liquid bath. The structure of the as-spun DES non-woven fabric fiber was changed to a crystallized form by immersion in a methanol solution, as portrayed in Fig. 4A. The isoelectronic solution of citric acid buffer at pH 3.8 can make the structure of WES non-woven fabric fibers crystallize without the following treatments. Comparison of the secondary structure contents between as-spun WES and methanol treated DES non-woven fabric fiber was performed by decomposition of each spectrum using curve-fitting technique. Lower ß-sheet

contents were estimated as as-spun WES non-woven fabric formed in citric acid buffer than as methanol-treated DES non-woven fabric (Fig. 4B). However, the ß-sheet content of WES non-woven fabric was increased with t-BuOH concentration and reached at the same level with the methanol treated DES non-woven fabric by 50% t-BuOH concentration (Fig. 4B). These results indicate that both isoelectronic solution and t-BuOH caused the crystallization of WES non-woven fabric in the coagulation bath when t-BuOH was mixed.

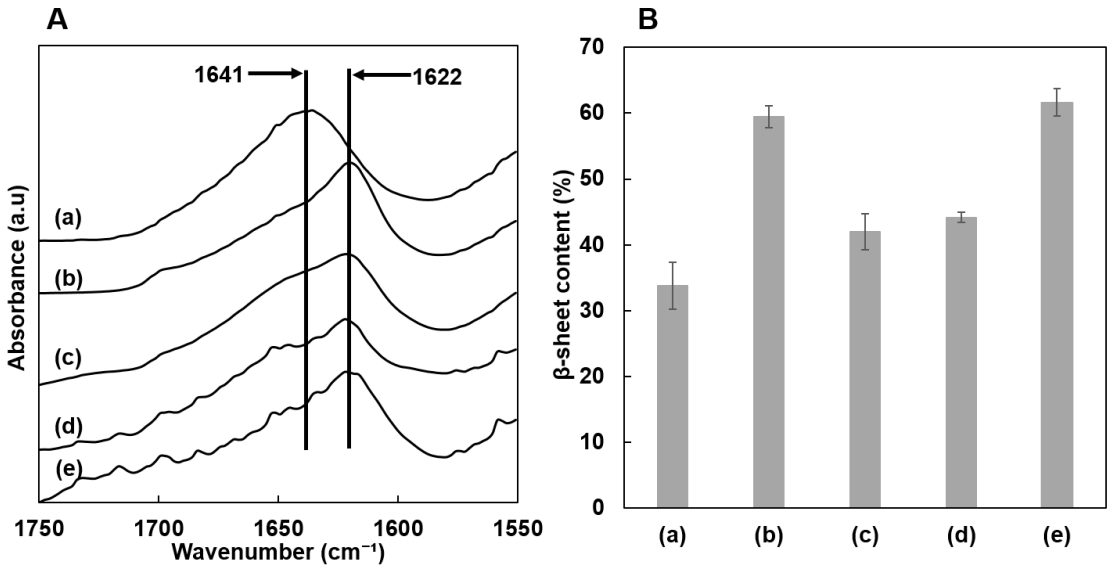


**Fig.4.** FTIR spectra and ß-sheet content of (a) as-spun DES non-woven fabric, (b) methanol treated DES non-woven fabric, (c) as-spun WES non-woven fabric formed in citric acid buffer at pH3.8, (d) with 30 vol%, and (e) 50 vol% of t-BuOH.
A: FTIR spectra.
B: ß-sheet content (n=3). ß-sheet content were calculated from areas of curve fitted peaks assigned to each conformation in the amide I region of the FTIR spectra. Error bars indicate the standard deviations.

### 3.4 Cell culture test

Figure 5 presents the initial cell adhesion and growth curve in/on the WES non-woven fabric using 30 vol% of t-BuOH, compared with those on the DES non-woven fabric. The initial cell adhesion on WES non-woven fabric was significantly lower than on DES fabric (Fig. 5A), but no difference of proliferation rates on the fabrics was observed (Fig. 5B). The pore size of the WES non-woven fabric used in cell culture was estimated as 12 μm. Furthermore, the apparent fiber density was much rougher than that of the DES non-woven fabric. Because the cell size is around 10 μm before adhesion, it will be harder for cells to be caught on the fiber matrix in the WES non-woven fabric than in the DES fabric. Therefore, the initial cell adhesion on WES non-woven fabric is expected to become lower than with DES non-woven fabric, which has much smaller pores and higher fiber density. Once the cells adhered on the SF nanofibers, cells were able to proliferate on the WES non-woven fabric at the same rate as on the DES non-woven fabric. These results mean that the cell growth was independent of the porosity or fiber density of the SF non-woven fabric.

Cell morphology on the DES and WES non-woven fabric using 30 vol% of t-BuOH, as discerned from SEM images, are depicted in Fig. 6. In the case of DES non-woven fabric, cells adhered only on the fabric surface with a well spreading shape. Then the fabric surface was covered fully with proliferated cells after 7 days of culture (Figs. 6(a) and 6(b)). In contrast, seeded cells adhered on both the surface and the inner spaces of WES non-woven fabric

during 1 day incubation (Fig. 6(c)) and proliferated on both the surface and the inner spaces of WES non-woven fabric after 7 days of culture (Fig. 6(d)). The cells in the WES non-woven fabric were spread along the SF nanofibers, resembling cross-linking members among the fibers. The proliferated cells into the inner spaces of WES fabric were clarified by observation of the cross section of the fabric cultured cells, as depicted in Figs. 6(e) and 6(f). Cells spread along the SF nanofibers into the fabric interior. The WES non-woven fabric was able to provide appropriate space and suitable support for 3D cell growth as a cell scaffold. It is anticipated for use as an extracellular matrix for tissue engineering.

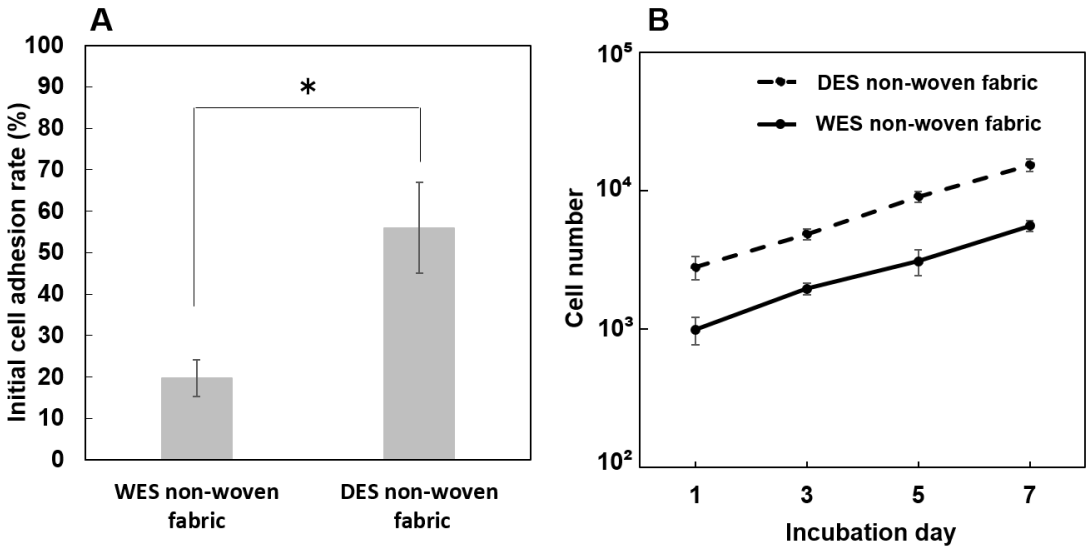


**Fig.5.** Initial cell adhesion rate and cell growth curve in/on WES and DES non-woven fabric. (A) Initial cell adhesion rate of after 1 day incubation, (B) Cell growth curve, (*, $p<0.05$ by t-test, n=3). T-test was employed to obtain p values, enabling determination of the level of significance of the data. P values of less than 0.05 was considered to be significant difference, and error bars indicate the standard deviations.

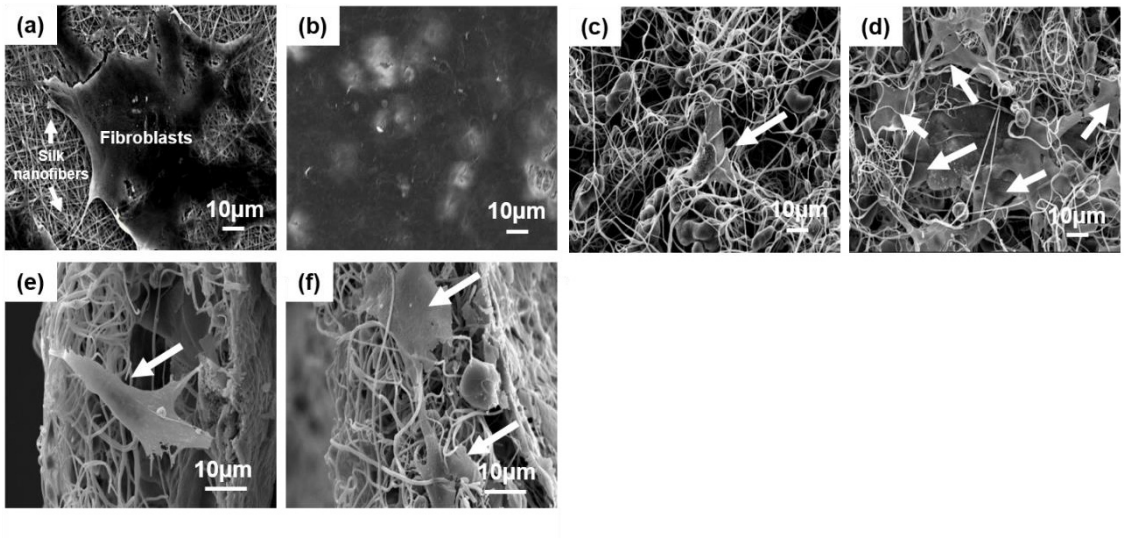


**Fig.6.** SEM images of cultured fibroblast cells on DES non-woven fabric after (a) 1 day, (b) 7 day and on WES non-woven fabric after (c) 1 day, (d) 7 day culture and cross sectional images of cultured fibroblast cells in WES non-woven fabric after (e) 5 day and (f) 7 day incubation.

## 4. Acknowledgment

This work was supported by JSPS KAKENHI Grant Number 26660265.

## 5. Reference

[1] J. G. Hardy, L. M. Romer, T. R. Scheibel, Polymeric materials based on silk proteins, Polymer, 49 (20) (2008) 4309–4327.

[2] B. Kundu, R. Rajkhowa, S. C. Kundu, X. Wang, Silk fibroin biomaterials for tissue regenerations, Adv. Drug. Deli. Rev., 65 (4) (2013) 457–470.

[3] S. D. Aznar-Cervantes, D. Vicente-Cervantes, L. Meseguer-Olmo, J. L. Cenis, A. A. Lozano-Perez, Influence of the protocol used for fibroin extraction on the mechanical properties and fiber sizes of electrospun silk mats, Mat. Sci. Eng. C, 33 (4) (2013) 1945–1950.

[4] H. J. Jin, J. Chen, V. Karageorgiou, G. H. Altman, D. L. Kaplan, Human bone marrow stromal cell responses on electrospun silk fibroin mats, Biomaterials, 25 (6) (2004) 1039–1047.

[5] H. Wang, Y. Zhang, H. Shao, X. Hu, Electrospun ultra-fine silk fibroin fibers from aqueous solutions, Journal of Materials Science, 40 (20) (2005) 5359–5363.

[6] J. Huang, L. Liu, J. Yao, Electrospinning of *Bombyx mori* silk Fibroin nanofiber mats reinforced by cellulose nanowhiskers, Fibers and Polymers, 12 (8) (2011) 1002–1006.

[7] N. Amiraliyan, M. Nouri, M. H. Kish, Structural characterization and mechanical properties of electrospun silk fibroin nanofiber mats[1], Polymer Science Series A, 52 (4) (2010) 407–412.

[8] Q. L. Loh, C. Choong, Three-Dimensional Scaffolds for Tissue Engineering Applications: Role of Porosity and Pore Size, Tissue. Eng. Part B., 19 (6) (2013) 485–502.

[9] H. S. Baek, Y. H. Park, C. S. Ki, J. C. Park, D. K. Rah, Enhanced chondrogenic responses of articular chondrocytes onto porous silk fibroin scaffolds treated with microwave-induced argon plasma, Surface and Coatings Technology, 202 (22–23),(2008) 5794–5797.

[10] S. Nedjari, G. Schlatter, A. Hebraud, Thick electrospun honeycomb scaffolds with controlled pore size, Materials Letters, 142 (2015) 180-183.

[11] S. Komura, T. Miyoshi, Japanese Patent 2007-217826-A (2007).

[12] Y. Ji, K. Ghosh, X. Z. Shu, B. Li, J. C. Sokolov, G. D. Prestwich, R. A. F. Clark, M. H. Rafailovich, Electrospun three-dimensional hyaluronic acid nanofibrous scaffolds, Biomaterials, 27 (20) (2006) 3782–3792.

[13] G. Kim, W. Kim, Highly porous 3D nanofiber scaffold using an electrospinning technique, J. Biomed. Mater. Res. Part B. Appl. Biomater., 81 (1) (2007) 104–110.

[14] Y. Yokoyama, S. Hattori, C. Yoshikawa, Y. Yasuda, H. Koyama, T. Takato, H. Kobayashi, Novel wet electrospinning system for fabrication of spongiform nanofiber 3-dimensional fabric, Materials Letters, 63 (9–10) (2009) 754–756.

[15] C. S. Ki, J. W. Kim, J. H. Hyun, K. H. Lee, M. Hattori, D. K. Rah, Y. H. Park, Electrospun Three-Dimensional Silk Fibroin Nanofibrous Scaffold, J. Appl. Polym. Sci., 106 (2007) 3922–3928.

[16] C. S. Ki, S. Y. Park, H. J. Kim, H. M. Jung, K. M. Woo, J. W. Lee, Y. H. Park, Development of 3-D nanofibrous fibroin scaffold with high porosity by electrospinning: implications for bone regeneration, Biotechnol. Lett., 30 (2008) 405–410.

[17] H. Dou, B. Zuo, Effect of sodium carbonate concentrations on the degumming and regeneration process of silk fibroin, The Journal of The Textile Institute, 106 (3) (2014) 311–319.

[18] Y. Kishimoto, H. Morikawa, S. Yamanaka, Y. Tamada, Electrospinning of silk fibroin from all aqueous solution at low concentration, Materials Science and Engineering C, 73 (2017) 498-506.

[19] O. N. Tretinnikov, Y. Tamada, Influence of Casting Temperature on the Near-Surface Structure and Wettability of Cast Silk Fibroin Films, Langmuir, 17 (23) (2001) 7406–7413.

[20] J. Zhu, Y. Zhang, H. Shao, X. Hu, Electrospinning and rheology of regenerated Bombyx mori silk fibroin aqueous solutions: The effects of pH and concentration, Polymer, 49 (12) (2008) 2880–2885.

[21] G. Vazquez, E. Alvarez, J. M. Navaza, Surface Tension of Alcohol Water + Water from 20 to 50°C, J. Chem. Eng. Data, 40 (3) (1995) 611–614.

[22] S. H. Kim, Y. S. Nam, T. S. Lee, W. H. Park, Silk Fibroin Nanofiber. Electrospinning, Properties, and Structure, Polymer Journal, 35 (2) (2003) 185–190.

# Chapter 5: Conclusion

## Chapter 5: Conclusion

In chapter: 2, I developed a new silk fibroin (SF)/ inorganic composite of electrospun SF nanofiber and montmorillonite (MMT), and characterized its microstructure. High-resolution TEM observations demonstrated that MMT layers, 1.2 nm thick were interacted in unknown way to the electrospun SF nanofibers covered with nanolayers of MMT. The nano SF/MMT composite were successfully fabricated using SF nanofiber, which had been immersed in MMT aqueous suspension. SF/MMT nanocomposite showed a circular cross-section and they possess 3 dimensional and high porosity structure. It is suggested that this nanocomposite is a candidate for new biocompatible application as scaffold for tissue engineering like bone regeneration, because the composite contain biodegradable and biocompatible silk and osteoinductive MMT and moreover the composite nanofiber may be advantageous scaffold in cell culture due to specially high surface area.

In chapter 3, SF non-woven mats were fabricated by electrospinning from all aqueous solution at low concentration (>5 wt %). Silk fibroin extracted from *Bombyx mori* silk cocoons by degumming using boiling water without alkaline reagents maintained a higher range of molecular weight distribution than fibroin that was degummed with alkaline. The spinning solution pH is important for electrospinning of a fibroin aqueous solution at low concentration. Results obtained from this study show that pH 10.5 is appropriate. The electrospinnability of aqueous fibroin solution depends on

the solution viscosity rather than the molecular weight of fibroin and the solution concentration. Mechanical properties of the non-woven mat depend on the fibroin molecular weight. The mean tensile stress and strain of the non-woven mat electrospun from the higher molecular weight fibroin were 0.83 ± 0.05 MPa / (g/m2) and 12 ± 5.6%.

In Chapter 4, I fabricated a three dimensional silk fibroin (SF) nanofiber non-woven fabric using wet electrospinning (WES) with SF aqueous spinning solution and a water based liquid bath. WES non-woven fabrics presents higher porosity than non-woven fabrics by traditional dry electrospinning (DES), with formed pores having maximum 12 μm average pore size. As-spun WES non-woven fabric fibers have a crystallized structure formed by spinning, whereas a non-crystallized structure was observed on the as-spun DES non-woven fabric. The initial cell adhesion was observed between WES and DES non-woven fabric. Cells were able to proliferate into WES non-woven fabrics, although cells on DES non-woven fabrics spread only on the fabric surface. The WES SF nanofiber non-woven fabric is anticipated for use as a cell scaffold to simulate an extracellular matrix structure.

# Chapter 6: Accomplishment

## 1. Journal of publications

[1] **Yuki Kishimoto**, Fuyu Ito, Hisanao Usami, Eiji Togawa, Masuhito Tsukada, Hideaki Morikawa, Sigeru Yamanaka, Nanocomposite of silk fibroin nanofiber and montmorillonite: Fabrication and morphology, International Journal of Biological and Macomolecules, 57 (2013) 124-128.

[2] **Yuki Kishimoto**, Takanori Kobashi, Hideaki Morikawa, Yasushi Tamada, Production of three-dimensional silk fibroin nanofiber non-woven fabric by wet electrospinning, Journal of Silk Science and Technology, Japan, 25 (2017) 49-57.

[3] **Yuki Kishimoto**, Hideaki Morikawa, Sigeru Yamanaka, Yasushi Tamada, Electrospinning of silk fibroin from all aqueous solution at low concentration, Materials Science and Engineering C, 73 (2017) 498-506.

## 2. Conferences

[1]Yuki Kishimoto, Hideaki Morikawa, Fabrication of electrospun silk fibroin nanofibers from silk fibroin aqueous solution, International Symposium on Fiber Science and Technology, (ISF2014), Tokyo, Japan, 2014.

[2]Yuki Kishimoto, Yasushi Tamada, Masuhiro, Tsukada, Sigeru Yamanaka, Hideaki Morikawa, Development of silk nanofiber: First report, Effect of degumming solution on electrospinnability, The 62th Conference on Japan Silk Science and Technology Japan, Okaya, Japan, 2015.

[3]Yuki Kishimoto, Yasushi Tamada, Masuhiro Tsukada, Sigeru Yamanaka, Hideaki Morikawa, Influence of degumming agent on the electrospinning ability of Bombyx mori silk fibroin aqueous solution, The 6th International Conference on Nanoscience & Technology, China ChinaNANO 2015, Beijing, Chana, 2015.

[4]Yuki Kishimoto, Masuhiro Tsukada, Yamanaka Tamada, Hideaki Morikawa, Study on mechanical properties of silk fibroin nanofiber non-woven mats, The 70th Fiber Preprints, Japan, Kyoto, Japan, 2015.

[5]Yuki Kishimoto, Yasushi Tamada, Sigeru Yamanaka, Hideaki Morikawa, Fabrication of silk fibroin nanofiber mat by wet electrospinning and analyze of properties, The 71th Fiber Preprints, Tokyo, Japan, 2016.

[6]**Yuki Kishimoto**, Hideaki Morikawa, Yasushi Tamada, Characterization of silk fibroin non-woven mats electrospun from formic acid and aqueous solution, 9th International Conference on Fiber and Polymer Biotechnology, Osaka, Japan 2016.

## 3. Patents

[1] Yasushi Tamada, **Yuki Kishimoto,** Hideaki Morikawa, Shigeru Yamanaka, Method for manufacturing three dimensional porous silk material, Japanese patent application No. 2016-173093.

[2] Yasushi Tamada, **Yuki Kishimoto**, Hideaki Morikawa, Shigeru Yamanaka , Method for manufacturing three dimensional silk material, Japanese patent application No. 2016-173094.

# Chapter 7: Acknowledgement

## Acknowledgment

It is my pleasure to write this message and express my gratitude to all those who have directly or indirectly contributed to the creation of this doctor dissertation. First of all I would like to thank my supervisor Professor Hideaki Morikawa and Professor Yasushi Tamada of Faculty of Textile Science and Technology, Shinshu University for giving me the opportunity to study in this study group and for always keeping me motivated and supporting me with a lot of useful advice. Special thanks are given to Professor Shigeru Yamanaka, Professor Yasuo Gotoh and Professor Masuhiro Tsukada of Faculty of Textile Science and Technology, Shinshu University

I would like to thank my colleagues in Morikawa Laboratory for their supports and helps and encourage me to finish this study.

I also would like to express my thanks to Tamada Laboratory students Mr. Kobashi, Mr. Sasaki, Ms. Watanabe, Mr. Ohtani and Mr. Sumi, who gave me many assistances, helps and helpful suggestions during my study life.

Finally, I dedicate my great thanks to my family and my parents.